Quantum Gravity, Séminaire Poincaré XXIV (2023) 33 – 64 Séminaire Poincaré

# Liouville quantum gravity and SLE

Jason Miller
DPMMS, University of Cambridge
Wilberforce Road, Cambridge
CB3 0WB, United Kingdom*

**Résumé.** We review recent developments in the mathematical study of Liouville quantum gravity and the Schramm-Loewner evolution and their application to the study of scaling limits of random planar maps.

## 1 Introduction

The purpose of this note is to survey recent developments in the subject of random planar geometry, focusing on the Schramm-Loewner evolution (SLE) and Liouville quantum gravity (LQG) and their application to the study of scaling limits of random planar maps (RPM). We note that there are a number of other excellent longer surveys and books on these topics [14, 22, 41, 70, 82, 92, 123, 136] to which we point the reader for a more in-depth overview. This note is structured as follows. We will first review SLE and how it arises as a scaling limit of the interfaces of lattice models in two-dimensional statistical mechanics in Section 2. We will then describe how SLE is coupled with the Gaussian free field (GFF) as a level line or flow line in Section 3. Next, we will give in Section 4 a brief review of RPM and their scaling limits. The purpose of Section 5 is to review LQG and in Section 6 we will review the construction of its metric. In Sections 5–6, we will also describe how LQG can be understood as a scaling limit of RPM. Finally, in Section 7 we will describe some recent developments which have combined the framework of SLE and LQG together with Liouville conformal field theory (LCFT) in order to determine a number of additional critical exponents and formulas for models which converge to SLE and related processes.

### Acknowledgements

The author was supported by ERC starting grant 804166 (SPRS).

## 2 The Schramm-Loewner evolution

The Schramm-Loewner evolution ($\mathrm{SLE}_\kappa$) was invented by Schramm in 1999 as a candidate to describe the scaling limits of different types of random planar curves which arise as interfaces in lattice models from statistical mechanics [116]. We will describe the complex analysis background necessary to define in SLE in Section 2.1. We will next give the definition of SLE in Section 2.2 and review some

*DPMMS, University of Cambridge, CB3 0WB, United Kingdom

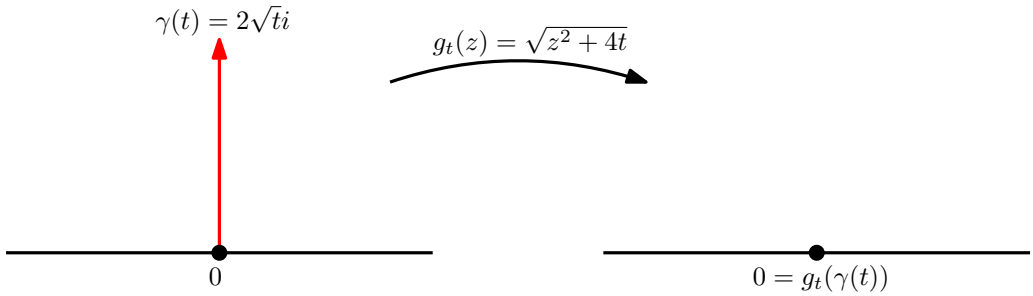


FIGURE 1 – Shown is the straight line $\gamma(t) = 2\sqrt{t}i$ in $\mathbf{H}$ from 0 to $\infty$ together with the unique conformal map $g_t(z)\colon \mathbf{H} \setminus \gamma([0,t]) \to \mathbf{H}$ with $g_t(z) - z \to 0$ as $z \to \infty$. Note that we explicitly have $g_t(z) = \sqrt{z^2 + 4t}$.

of the results which have been proved about the sample path properties of SLE. Finally, in Section 2.3 we will describe how SLE arises as a scaling limit of the interfaces in several lattice models.

### 2.1 Chordal Loewner equation

The starting point to define SLE is the chordal Loewner equation, which has its roots in work of Loewner from the 1920s [87] in his efforts to prove the Bieberbach conjecture concerning the growth of the coefficients in the power series expansion of a univalent function. The Bieberbach conjecture was ultimately proved in 1985 by de Branges [26] and his proof makes use of Loewner evolutions; see [130] for a self-contained treatment.

Recall that $K \subseteq \mathbf{H}$ is called a *compact* $\mathbf{H}$*-hull* if $\overline{K}$ is compact and $\mathbf{H} \setminus K$ is simply connected. If $K \subseteq \mathbf{H}$ is a compact $\mathbf{H}$-hull, then it is not difficult to show that there exists a unique conformal map $g_K\colon \mathbf{H} \setminus K \to \mathbf{H}$ such that $g_K(z) - z \to 0$ as $z \to \infty$. The *chordal Loewner equation* serves to encode a "continuously" and "locally" growing family of compact $\mathbf{H}$-hulls $(K_t)$, which could correspond to a non-crossing curve in $\mathbf{H}$ from 0 to $\infty$, in terms of the evolution of the conformal maps $(g_t) = (g_{K_t})$ which in turn are the solution of a simple ODE.

The simplest example is the vertical line $K_t = [0, 2\sqrt{t}i]$ in $\mathbf{H}$ from 0 to $\infty$ (we will momentarily explain the reason for this choice of time parameterization). It is not difficult to see in this case that $g_t = g_{K_t}$ is given by $z \mapsto \sqrt{z^2 + 4t}$. Observe that

$$\partial_t g_t(z) = \frac{4}{2\sqrt{z^2 + 4t}} = \frac{2}{g_t(z)}, \quad g_0(z) = z. \tag{1}$$

Since the ODE $\partial_t g_t(z) = 2/g_t(z)$, $g_0(z) = z$ from (1) has a unique solution for each fixed $z \in \mathbf{H}$ up until the time $\tau_z = \inf\{t \geq 0 : \mathrm{Im}(g_t(z)) = 0\}$ it follows that the ODE itself encodes the family of conformal maps $(g_t)$ hence the vertical line $(K_t)$ itself.

Let us now make a comment about the geometric interpretation of the choice of time parameterization for $(K_t)$. It is not difficult to see that for a compact $\mathbf{H}$-hull $K$ the conformal map $g_K$ admits the Laurent expansion

$$g_K(z) = z + \sum_{k=1}^{\infty} \frac{b_k}{z^k} \quad \text{as} \quad z \to \infty. \tag{2}$$

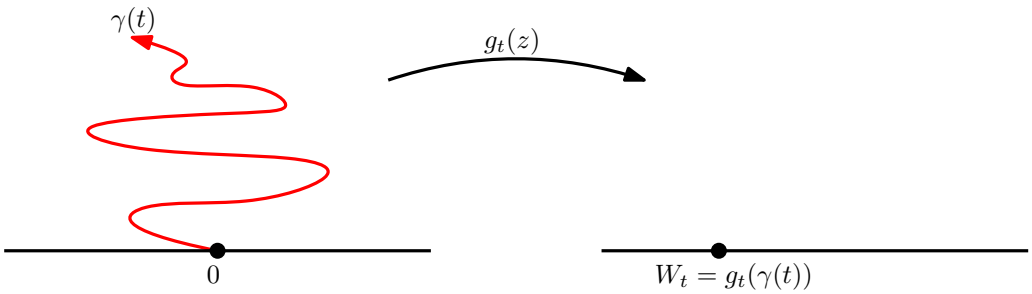


Figure 2 – Shown is the setup for Loewner's theorem in the context of a non-self-crossing curve $\gamma$ in $\mathbf{H}$ from 0 to $\infty$. For each $t \geq 0$, $g_t$ is the unique conformal map from the unbounded component $\mathbf{H}_t$ of $\mathbf{H}\backslash\gamma([0,t])$ to $\mathbf{H}$ with $g_t(z) - z \to 0$ as $z \to \infty$. In this case, the driving function $W$ in the chordal Loewner equation satisfies $W_t = g_t(\gamma(t))$ for each $t \geq 0$.

The coefficient $b_1$ from (2) is the called the *half-plane capacity* of $K$ and is denoted by $\mathrm{hcap}(K)$. Equivalently,

$$\mathrm{hcap}(K) = \lim_{y\to\infty} y\mathrm{Im}(iy - g_K(iy)). \tag{3}$$

Using (3), one can also see that

$$\mathrm{hcap}(K) = \lim_{y\to\infty} y\mathbf{E}_{iy}[\mathrm{Im}(B_\tau)] \tag{4}$$

where $B$ is a standard Brownian motion in $\mathbf{C}$, $\mathbf{E}_{iy}$ denotes the expectation under the law with $B_0 = iy$, and $\tau = \inf\{t \geq 0 : B_t \notin \mathbf{H} \setminus K\}$. From (3), one can see that the time parameterization of the line $K_t$ is such that

$$\mathrm{hcap}(K_t) = 2t \quad \text{for all} \quad t \geq 0. \tag{5}$$

This is the so-called *half-plane capacity parameterization* and this choice makes the form of the ODE (1) that $(g_t)$ solves particularly simple.

The idea of the Loewner evolution is to extend this encoding of the vertical line in terms of an evolving family of conformal maps to the setting of any family $(K_t)$ of compact $\mathbf{H}$-hulls which grow *continuously* (meaning that we can reparameterize time so that $(K_t)$ is parameterized by half-plane capacity (5)) and *locally* (meaning that $g_t = g_{K_t}$ satisfies $\mathrm{diam}(g_t(K_{t+\delta})) \to 0$ as $\delta \to 0$ uniformly in $0 \leq t \leq T$ for each fixed $T > 0$). Suppose that $(K_t)$ is a locally growing family of compact $\mathbf{H}$-hulls which are parameterized by half-plane capacity and $g_t = g_{K_t}$ for each $t \geq 0$. Then the result is that there exists a continuous function $W\colon \mathbf{R}_+ \to \mathbf{R}$ so that the family $(g_t)$ solves the *chordal Loewner equation*

$$\partial_t g_t(z) = \frac{2}{g_t(z) - W_t}, \quad g_0(z) = z. \tag{6}$$

The function $W$ is called the *driving function* for $(K_t)$. Note that in the case of the vertical line we have that $W \equiv 0$. Conversely, suppose that $W\colon \mathbf{R}_+ \to \mathbf{R}$ is continuous and $(g_t)$ denotes the solution to (6) which for each $z \in \mathbf{H}$ is defined up to $\tau_z = \inf\{t \geq 0 : \mathrm{Im}(g_t(z)) = 0\}$. Let $\mathbf{H}_t = \{z \in \mathbf{H} : \tau_z > t\}$ and $K_t = \mathbf{H} \setminus \mathbf{H}_t$. Then $(K_t)$ is a locally growing family of compact $\mathbf{H}$-hulls which are parameterized

by half-plane capacity and for each $t \geq 0$ we have that $g_t$ is the unique conformal map $\mathbf{H}_t \to \mathbf{H}$ with $g_t(z) - z \to 0$ as $z \to \infty$.

Such a family $(K_t)$ is said to be *generated by a continuous curve* if there exists $\gamma \colon \mathbf{R}_+ \to \overline{\mathbf{H}}$ so that $K_t$ is the complement in $\mathbf{H}$ of the unbounded component of $\mathbf{H} \setminus \gamma([0,t])$ for each $t \geq 0$. In this case, we have that $W_t = g_t(\gamma(t))$ for each $t \geq 0$. It has been shown that there exists a constant $C > 0$ so that if $W$ is 1/2-Hölder continuous with 1/2-Hölder norm at most $C$ then the corresponding $(K_t)$ is generated by a continuous curve but there are examples of $W$ which are 1/2-Hölder continuous so that the corresponding $(K_t)$ is not generated by a continuous curve [89].

## 2.2 Schramm-Loewner evolution

We will now give the definition of the Schramm-Loewner evolution (Section 2.2.1) and then review some of the results which have been established for its sample path properties (Section 2.2.2).

### 2.2.1 Definition

Suppose that $\kappa \geq 0$. The Schramm-Loewner evolution ($\mathrm{SLE}_\kappa$) is the random family $(K_t)$ of compact $\mathbf{H}$-hulls arising by solving (6) with the particular choice $W = \sqrt{\kappa} B$ where $B$ is a standard Brownian motion. This form of $W$ was derived by Schramm [116] from the so-called *conformal Markov property*, which states that if $(K_t)$ is a random family of compact $\mathbf{H}$-hulls which arise as the scaling limit of an interface from a two-dimensional lattice model which is conformally invariant in the scaling limit then :

(i) For each fixed $s \geq 0$, $t \mapsto g_s(K_{t+s}) - W_s \overset{d}{=} (K_t)$ and

(ii) For each $\alpha \geq 0$, $(\alpha^{-1} K_{\alpha^2 t}) \overset{d}{=} (K_t)$.

Indeed, (i) implies that $W$ has stationary and independent increments hence must be of the form $\sqrt{\kappa} B_t + at$ where $B$ is a standard Brownian motion, $\kappa \geq 0$, and $a \in \mathbf{R}$. Moreover, (ii) implies that $W$ satisfies Brownian scaling hence $a = 0$. Beyond its simplicity, what is remarkable about the definition of $\mathrm{SLE}_\kappa$ is that one can apply the tools of stochastic calculus to (6) to establish many of its properties.

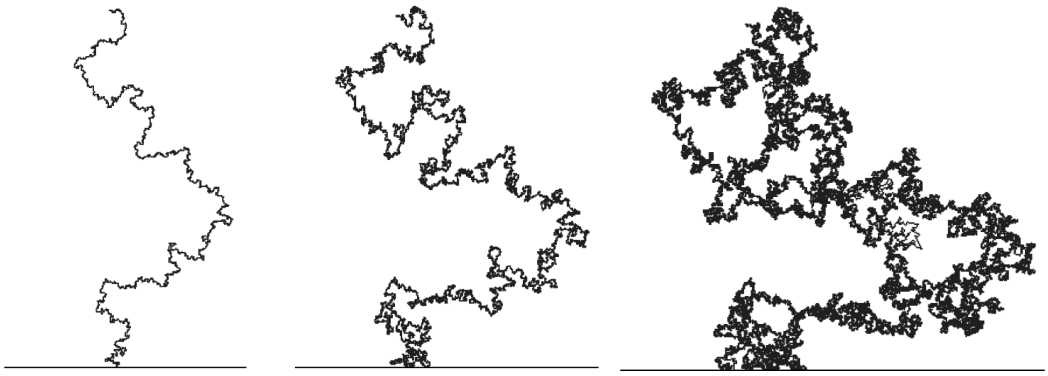

FIGURE 3 – Numerical simulations due to Tom Kennedy. **Left :** $\mathrm{SLE}_2$. **Middle :** $\mathrm{SLE}_4$. **Right :** $\mathrm{SLE}_6$.

#### 2.2.2 Sample path properties

Since $B$ is not 1/2-Hölder continuous, one cannot make use of the deterministic theory mentioned above to show that $\mathrm{SLE}_\kappa$ is generated by a continuous curve. The existence of the $\mathrm{SLE}_\kappa$ curve was proved by Rohde-Schramm for $\kappa \neq 8$ [114] and by Lawler-Schramm-Werner for $\kappa = 8$ [76] as a consequence of the convergence of the uniform spanning tree Peano curve to $\mathrm{SLE}_8$ (see also [4] for a proof of the convergence which does not make use of discrete models). The *phases* of $\mathrm{SLE}_\kappa$ were also determined by Rohde-Schramm and the underlying calculation is often one of the first that one sees when learning about $\mathrm{SLE}_\kappa$. It is based on the observation that for each $x \in \mathbf{R}$ we have that $g_t(x) - W_t$ evolves as a multiple of a Bessel process, so the phases can be determined using basic properties of Bessel processes. In particular, $\mathrm{SLE}_\kappa$ is a simple curve for $\kappa \in (0, 4]$, self-intersecting but not space-filling for $\kappa \in (4, 8)$, and space-filling for $\kappa \geq 8$. The Hausdorff dimension of the range of an $\mathrm{SLE}_\kappa$ curve was computed in [10, 114] and is $\min(1 + \kappa/8, 2)$. In the case that $\kappa \in (0, 8)$ (resp. $\kappa > 4$), $\mathrm{SLE}_\kappa$ curves have cut (resp. double) points and the dimension of such points was determined in [105].

Many other works have explored the sample path properties of SLE. For example, the optimal Hölder exponent for the SLE curve with the capacity parameterization was determined in [56, 86]. The optimal Hölder exponent vanishes for $\kappa = 8$ and in this case the modulus of continuity is given by $(\log \delta^{-1})^{-1/4+o(1)}$ as $\delta \to 0$ [60]. The regularity of the $\mathrm{SLE}_\kappa$ curve is closely related to the behavior of harmonic measure near the tip of the curve and this was explored in detail in [57] in which the multi-fractal spectrum near the tip was determined. The optimal Hölder exponent for the uniformizing maps $(g_t)$ away from the tip was determined in [51] and this is closely related to the behavior of harmonic measure of the SLE curve away from the tip. The Hölder exponent for the uniformizing map vanishes for $\kappa = 4$ and the modulus of continuity in this case is given by $(\log \delta^{-1})^{-1/3+o(1)}$ as $\delta \to 0$ [60]. Further papers have explored many other regularity properties of the $\mathrm{SLE}_\kappa$ curves, for example the so-called *integral means spectrum* was computed in [11] (in expectation) and in [51] (almost surely).

Implicit in the definition of $\mathrm{SLE}_\kappa$ using the chordal Loewner equation (6) is a direction of time : the curve naturally grows from 0 to $\infty$ in $\mathbf{H}$. However, as $\mathrm{SLE}_\kappa$ arises or is conjectured to arise as the scaling limit of many different two-dimensional lattice models for which the interfaces do not have a direction of time it is natural to expect that it possesses the following time-reversal symmetry property : if $\eta$ is an $\mathrm{SLE}_\kappa$ in $\mathbf{H}$ from 0 to $\infty$, then up to a monotone reparameterization of time with $\psi(z) = \overline{z}^{-1}$ (where $\overline{z}$ denotes the complex conjugate of $z$) we have that $\psi(\eta) \overset{d}{=} \eta$. The time-reversal symmetry of $\mathrm{SLE}_\kappa$ is not obvious from its definition in terms of (6). It was first proved by Zhan [138] for $\kappa \in (0, 4]$ (see also [30, 94]) and for $\kappa \in (4, 8]$ in [95]. For $\kappa > 8$, the $\mathrm{SLE}_\kappa$ curves do not satisfy time-reversal symmetry but it is nevertheless possible to give an explicit description of their time-reversal and it is an $\mathrm{SLE}_\kappa$-type curve [97].

The capacity time parameterization for $\mathrm{SLE}_\kappa$ is natural from its definition in terms of the chordal Loewner equation (6), but it is not natural from the perspective of it as the scaling limit of discrete models. Indeed, in the case of a discrete lattice model it is natural to parameterize a curve by the number of edges or vertices that it traverses. The *natural parameterization* of $\mathrm{SLE}_\kappa$ was first constructed in [78] and

is a continuum time parameterization for $\mathrm{SLE}_\kappa$ which conjecturally describes the scaling limit of a discrete model with the edge parameterization. The construction given in [78] is indirect but it was subsequently shown in [71] that the natural parameterization corresponds to parameterizing $\mathrm{SLE}_\kappa$ by Minkowski content.

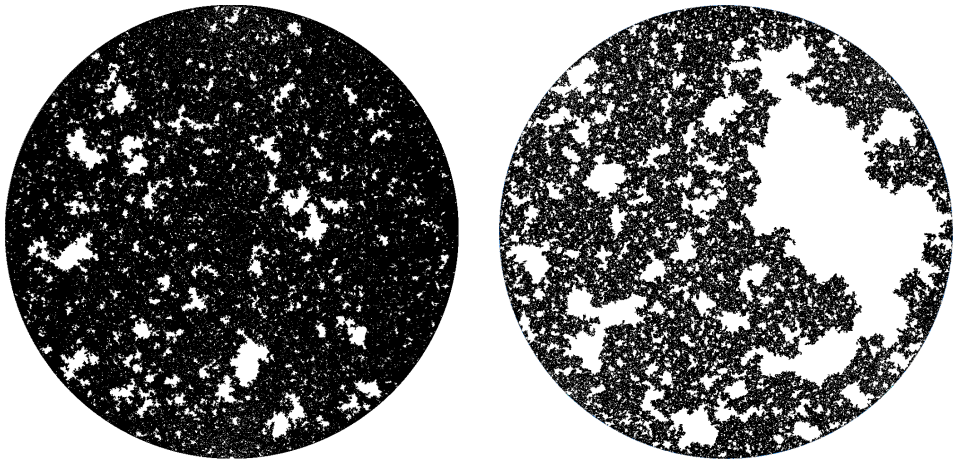

FIGURE 4 – Numerical simulations of CLE. **Left :** $\mathrm{CLE}_3$. **Right :** $\mathrm{CLE}_6$.

As we will describe below, $\mathrm{SLE}_\kappa$ serves to describe the scaling limit of a single interface from a discrete model. The *conformal loop ensembles* ($\mathrm{CLE}_\kappa$) are the loop version of $\mathrm{SLE}_\kappa$ and serve to describe the scaling limit of all of the interfaces [120, 124].

Since the discovery of $\mathrm{SLE}_\kappa$, there are now several different constructions which are useful in its study depending on the type of problem that one is considering :

(i) The chordal Loewner equation (6).
(ii) The outer boundary of Brownian motion or a cluster of Brownian loops from the Brownian loop-soup (see Section 2.3).
(iii) The level or flow line of the GFF (see Section 3).
(iv) The conformal welding and mating of trees representations (see Section 5.3).

### 2.3 Convergence results on planar lattices

Many two-dimensional lattice models at criticality from statistical mechanics have been conjectured to be *conformally invariant* in the scaling limit. This is in fact natural to expect because the scaling limit of the infinite volume limit of such a model should be :

— Translation invariant as translation invariance persists in the scaling limit.
— Scale invariant as it is a scaling limit.
— Rotationally invariant if the underlying lattice has sufficient symmetry.

Such models also often satisfy a natural Markov property which altogether turns into the scaling limit satisfying the conformal Markov property which characterizes $\mathrm{SLE}_\kappa$.

We will first explain how this works in the context of the critical percolation model on the triangular lattice. Fix $n \in \mathbf{N}$ and suppose that $\mathcal{T}_n$ is an $n \times n$ "lozenge"

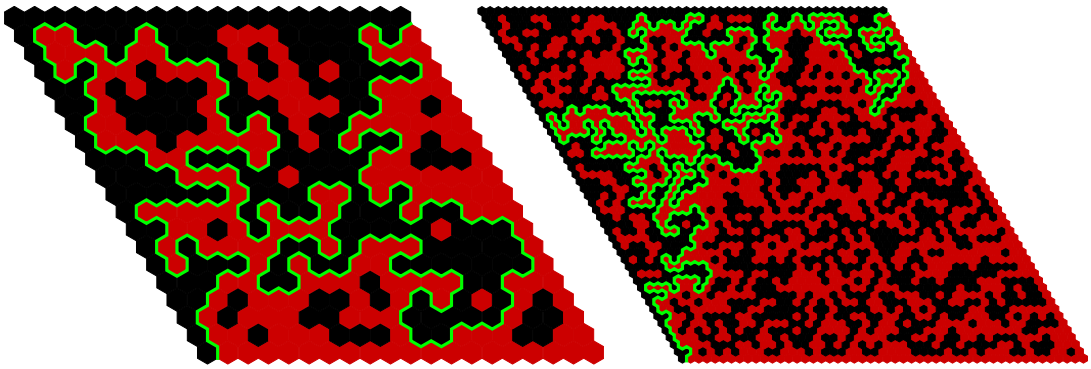

FIGURE 5 – Critical percolation ($p = 1/2$) on part of the triangular lattice (with vertices represented by hexagons) with black (resp. red) boundary conditions on the left (resp. right) and top (resp. bottom) boundary. The interface from the bottom left to top right with black (resp. red) hexagons on its left (resp. right) is shown in green. **Left :** Simulation on a $20 \times 20$ part of the triangular lattice. **Right :** Simulation on a $50 \times 50$ part of the triangular lattice.

of the triangular lattice as illustrated in Figure 5, where each vertex in the triangular lattice is represented by a hexagon. Each hexagon is then colored either black or red based on the toss of an independent fair coin flip, where the hexagons on the left (resp. right) and top (resp. bottom) part of the boundary are colored black (resp. red). This forces the existence of a unique interface starting from the bottom left part of the lozenge to the top right which has the property that the hexagons to its left (resp. right) are black (resp. red). It was proved in [17, 125] that in the scaling limit this interface converges to an $\mathrm{SLE}_6$ curve. As a consequence of this, using computations in the continuum with $\mathrm{SLE}_6$ it has been possible to verify many conjectures previously made about the scaling limit of critical percolation (e.g., [127]).

Similar scaling limit results have been proved for a number of other models, for example the Ising and FK Ising model [13, 20, 63, 126], the contours of the discrete Gaussian free field [117], and the uniform spanning tree Peano curve and loop-erased random walk trajectory [76] (see Figure 6 for an illustration). A number of other models have been conjectured to converge to $\mathrm{SLE}_\kappa$ in the scaling limit, including the FK model for general values of $q$ [120], the self-avoiding walk model (SAW) [77], and bipolar orientations [66].

Another famous application of the SLE curves was the computation of the *Brownian intersection exponents*, which give the probability that $k$ independent Brownian motions starting from equally spaced points on $\partial B(0, \epsilon)$ reach $\partial B(0, 1)$ without intersecting each other [72–75]. This, in turn, was used to verify Mandelbrot's conjecture which states that the outer boundary of a planar Brownian motion (see Figure 6) has dimension 4/3.

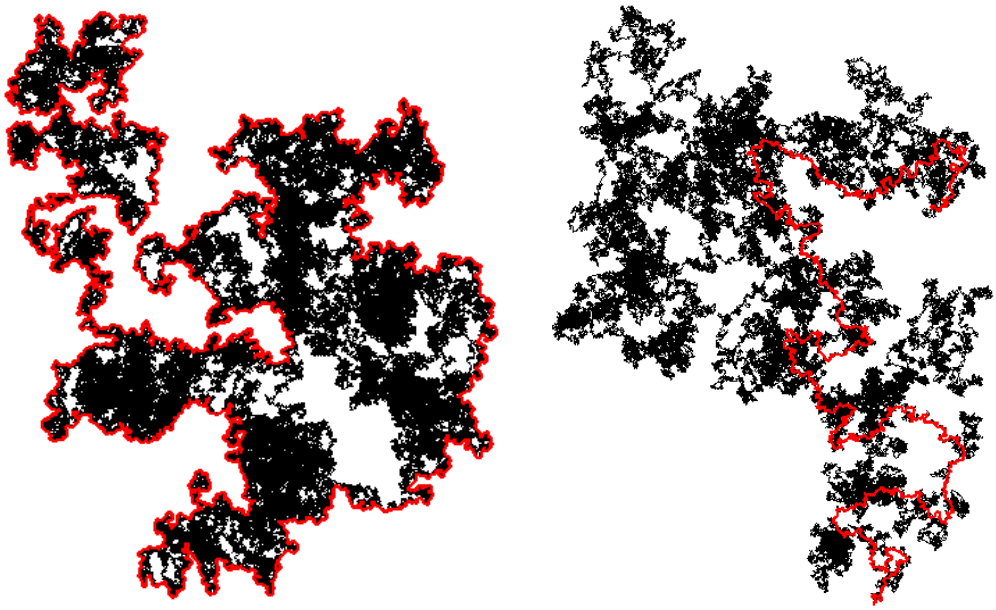

FIGURE 6 – **Left :** Outer boundary of a planar Brownian motion. **Right :** Random walk (black) together with its loop-erasure (red).

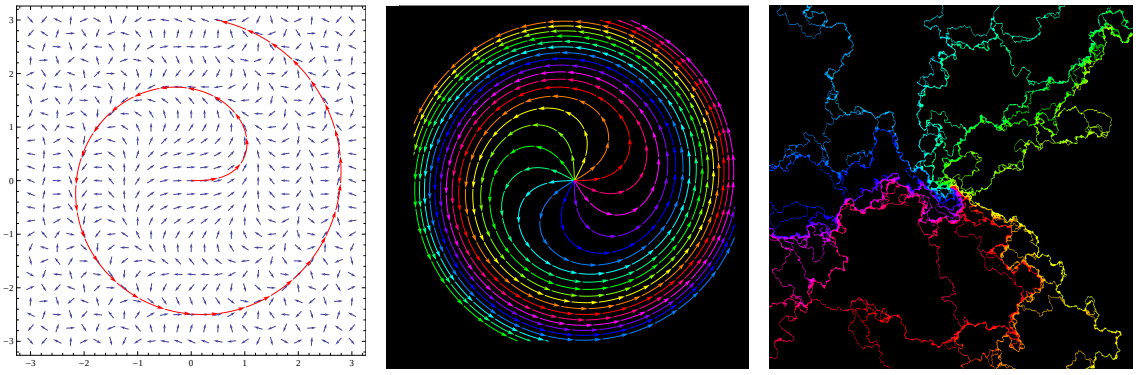

FIGURE 7 – **Left :** The vector field $e^{ih(z)}$ where $h(z) = x^2 + y^2$ together with the flow line with angle zero starting from the origin. **Middle :** The same vector field as on the left with 12 flow lines starting from the origin with equally spaced angles. **Right :** Numerically generated flow lines of $e^{ih/\chi}$ where $h$ is a discrete approximation of the GFF, $\chi = 2/\sqrt{\kappa} - \sqrt{\kappa}/2$ and $\kappa = 4/3$, and with equally spaced angles.

## 3 Level lines and flow lines of the GFF

In this section we will describe one of the other ways of constructing SLE curves using the Gaussian free field (GFF). This perspective has been useful for proving a number of results about SLE which seem to be difficult to establish based on its definition in terms of the chordal Loewner equation (6). Let us begin by reviewing the definition of the GFF. (For the reader who is interested in more details, there are many excellent surveys on the GFF including [119, 137].) Suppose that $D \subseteq \mathbf{C}$ is a domain. The GFF $h$ on $D$ with zero boundary conditions is the mean zero Gaussian field with covariance function given by the Green's function $G$ for $\Delta$ on $D$ with

Dirichlet boundary conditions. Since $G(x,y) \sim -\log|x-y|$ as $x \to y$, the GFF has infinite variance at points and as result takes values in the space of distributions in the sense of Schwartz rather than in the space of functions. One way of constructing the GFF is to view it as the standard Gaussian associated with the Hilbert space $H_0^1(D)$, which is the Hilbert space closure of $C_0^\infty(D)$ with respect to the *Dirichlet inner product*

$$(f,g)_\nabla = \frac{1}{2\pi}\int \nabla f(x)\cdot\nabla g(x)dx. \tag{7}$$

If $(\phi_n)$ is an orthornomal basis of $H_0^1(D)$ and $(\alpha_n)$ is a sequence of i.i.d. $N(0,1)$ random variables, then $h$ admits the series expansion

$$h = \sum_n \alpha_n \phi_n. \tag{8}$$

This series does not converge in $H_0^1(D)$ (it is immediate that the $\|\cdot\|_\nabla$-norm of the partial sums in (8) blows up), but it does converge in $H^{-\epsilon}(D)$ for every $\epsilon > 0$. That is, the GFF is not a function valued random variable but it is arbitrarily close to being in $L^2(D)$. This is a reflection of the fact that the covariance function only blows up logarithmically (and not polynomially) on the diagonal. More generally, the GFF with boundary conditions $\phi$ on $\partial D$ is equal to the sum of a GFF with zero boundary conditions on $D$ and the function $\mathfrak{h}$ which is harmonic on $D$ with $\mathfrak{h}|_{\partial D} \equiv \phi$.

The GFF arises in many contexts in probability theory, for example describing the fluctuations of random surfaces and height functions [64,65,112], its connection to random walk and Brownian motion through isomorphism theorems [129], and as a building block for various random geometries. We will describe how this works in the context of SLE in this section and for the Liouville quantum gravity surfaces in Section 5.

Since the Green's function is conformally invariant (equivalently, (7) is conformally invariant), the GFF is conformally invariant as well. Moreover, the GFF satisfies the following spatial Markov property : if $U \subseteq D$ is open, then we can write $h = h_1 + h_2$ where $h_1$ is a GFF on $U$ with zero boundary conditions, $h_2$ is distribution on $D$ which is harmonic in $U$, and $h_1, h_2$ are independent. This can be seen because $H_0^1(D)$ admits the orthogonal decomposition $H_1(U) \oplus H_2(U)$ where $H_1(U) = H_0^1(U)$ (resp. $H_2(U)$) consists of those functions in $H_0^1(D)$ which are supported (resp. harmonic) in $U$. Together, the conformal invariance and spatial Markov property of the GFF are analogous to the conformal Markov property which characterizes SLE. As a result, SLE and the GFF are deeply connected.

Since the GFF is not (but is very close to being) function valued, it exhibits many properties that functions have but with an extra "twist" to reflect the fact that it is not a function. One important example of this was discovered by Schramm and Sheffield [117,118] in which they showed that it is possible to make sense of the level sets of the GFF and they are $\mathrm{SLE}_4$-type curves. Since the GFF is a distribution, this construction is non-trivial. So far, two approaches have been developed. The first construction is the focus of [117] in which it is shown that the level sets for an approximation of the GFF based on the GFF defined on a lattice approximation of $D$ converge in the scaling limit. There are many other natural approximations of the GFF, for example by integrating it against a mollifying function, but to do date it has not been proved that the corresponding level sets converge. The second construction

is the focus of [118]. It is indirect and takes place purely in the continuum without using an approximation procedure for the GFF. It is based on "reverse engineering" what it would mean for a curve to be a level set of the GFF and then proving its existence using the tools of stochastic calculus.

This construction was extended by Sheffield [121] (see also [31]) in which he showed that it is possible to make sense of the formal solutions to the equation

$$\frac{d}{dt}\eta(t) = e^{ih(\eta(t))/\chi} \quad \text{where} \quad \chi = \frac{2}{\sqrt{\kappa}} - \frac{\sqrt{\kappa}}{2} \quad \text{for} \quad \kappa \in (0,4) \tag{9}$$

and the solutions are $\mathrm{SLE}_\kappa$ curves. See Figure 7 for an illustration. In (9), the expression $e^{ih/\chi}$ should be thought of as a random vector field which is generated by the GFF and $\eta$ is a flow line of this vector field. Since the GFF is a distribution, but not a function, this expression does not make literal sense. It is expected that these flow lines arise by mollifying the GFF, solving the corresponding equation, and then taking a limit. This approach, however, has not yet been proved to work. The construction given in [121] is indirect, takes place in the continuum without approximating the GFF, and uses the tools of stochastic calculus as in [118]. The $\mathrm{SLE}_{\kappa'}$ curves with $\kappa' = 16/\kappa$ also naturally arise in this framework but their interpretation is different as they do not correspond to a single flow line but rather a "tree" of flow lines. This is closely related to the fact that with $\chi$ as in (9) we have that $\chi(\kappa') = -\chi(\kappa)$.

The theory of how these flow lines interact with each other is developed in [31, 93] (in the case that the flow lines start from boundary points) and in [97] (in the case that the flow lines start from interior points). They exhibit many of the same properties that flow lines of a smooth vector field have both in terms of their behavior and their interaction with each other. For example, for each $\theta$ one can define the flow line of angle $\theta$ to be the flow line of $h + \theta\chi$ (so that when considering $e^{i(h+\theta\chi)/\chi} = e^{i(h/\chi+\theta)}$ all of the arrows are rotated by the angle $\theta$). Suppose that $\eta_1, \eta_2$ are flow lines with angles $\theta_1, \theta_2$ where $\eta_1$ starts to the left of $\eta_2$. When $\theta_1 > \theta_2$, we have that $\eta_1$ stays to the left of $\eta_2$. When $\theta_2 - \pi < \theta_1 < \theta_2$, $\eta_1$ crosses $\eta_2$ and cannot subsequently cross back. In contrast to the case of a smooth vector field, if $\theta_1$ is sufficiently close to $\theta_2$, then $\eta_1$ can in fact bounce off $\eta_2$ upon intersecting for the first time and the subsequent intersections form a fractal and uncountable set. If $\theta_1 = \theta_2$, then $\eta_1$ will merge with $\eta_2$ so that flow lines with the same angle form a tree structure. The theory of the GFF flow lines have many applications to solving SLE problems [94, 95]. See also [135] in which the theory of how the level lines of the GFF interact is developed.

## 4 Random planar maps

### 4.1 Overview and definitions

We now turn to describe the so-called *random planar maps* (RPM). Recall that a *planar map* is a graph together with an embedding into the plane so that no two edges cross. Two planar maps are considered to be equivalent if there exists an orientation preserving homeomorphism of the plane which takes one to the other. We note that this is a stronger condition than requiring the underlying graphs to be isomorphic. The *faces* of a planar map are the connected components of the

complement of its edges. The *degree* of a face is the number of adjacent edges. A map is called a *triangulation* (resp. *quadrangulation*) if all of its faces have degree 3 (resp. 4). In general, one can study planar maps where all of the faces have a fixed degree $p$ (called a *$p$-angulation*) and also the case where the face degrees are mixed. The study of planar maps has its roots in work of Tutte [131–134] and Mullin [106] from the 1960s in their work on the question of enumerating planar maps.

RPM are random graphs on which one can consider the statistical mechanics models that we mentioned in Section 2. It turns out that it is easier to study these models on RPM in comparison to deterministic planar lattices like $\mathbf{Z}^2$ or the triangular lattice provided the law of the RPM is chosen properly. The reason for this is that one can imagine exploring an interface of e.g. the percolation model as illustrated in Figure 5. If the underlying graph is fixed, then the conditional law of the remaining percolation configuration depends on the *shape* of the interface which has been observed. On the other hand, for an appropriately chosen model of RPM the underlying graph is random and the conditional law of what remains will depend only on the boundary lengths of the complementary components of the interface (number of edges on the boundary). If one focuses on the component that the interface is traversing, this is a one-dimensional quantity which results in a Markov chain which is tractable to study. In particular, if one considers certain setups it is often possible to have that the boundary length evolution process has i.i.d. increments so in the scaling limit is described by Lévy process or even a Brownian motion. From the evolution of the boundary length process, one can extract many properties of the statistical mechanics model on the planar map including its critical exponents. The critical exponents associated with a given model (e.g., percolation) on a RPM are different from the corresponding exponents on a deterministic planar lattice (e.g., the triangular lattice). However, they turn out to be related by the KPZ formula which serves to take into account the comparison between the Euclidean metric and the graph metric for a RPM when the latter is embedded into the plane in a conformal manner. This is one of the methods that physicists used to (non-rigorously) predict these exponents which mathematicians were later able to verify using SLE. We will discuss the KPZ formula in more detail in Section 5.

### 4.2 Uniformly random planar maps

Let us first describe some of the work which has been done on RPM which are chosen *uniformly* at random among the set of $p$-angulations with a fixed number of faces. Let $\mathbf{Q}_n^\bullet$ be the set of quadrangulations which are marked by a distinguished vertex (called the *root*) and a distinguished oriented edge (called the *dual root*). There is a remarkably simple formula for $|\mathbf{Q}_n^\bullet|$ due to Tutte :

$$|\mathbf{Q}_n^\bullet| = \frac{2 \cdot 3^n}{n+1} \binom{2n}{n}. \tag{10}$$

A bijective proof of (10) was derived in the work of Cori-Vauquelin [21] and Schaeffer [115] (now called the *CVS bijection*) which serves to encode such a quadrangulation in terms of a so-called *well-labeled tree*. This is simply a rooted plane tree where each vertex has a label in $\mathbf{Z}$, the root has label 0, and the labels of adjacent vertices differ by at most 1. From this perspective, the enumeration formula (10) immediately follows since the number of rooted plane trees with $n$ edges is given by the $n$th

Catalan number and the number of well-labelings of such a tree is $3^n$. Since there are only finitely many such possibilities, one can choose such a quadrangulation (or equivalently a well-labeled tree) uniformly at random. We note that one can sample from the law of a uniformly random well-labeled tree $\mathcal{T}$ by first sampling the tree uniformly at random from the set of plane trees with $n$ edges and then given $\mathcal{T}$ sampling the labels uniformly at random. The former corresponds to an excursion of a simple random walk in $\mathbf{Z}$ with $2n+1$ steps starting from 0 and conditioned to hit $-1$ for the first time at time $2n+1$ and the latter corresponds to a collection of random walks on the branches of $\mathcal{T}$ which start from 0 at the root, have increments $-1$, 0, and 1 with equal probability, and are coupled together to be the same when two branches agree but evolve independently after they first separate. In the CVS bijection, the vertices of the rooted quadrangulation are equal to the vertices of the tree together with an extra vertex $v_*$ which is the root of the quadrangulation. One then assigns $v_*$ the label $\ell_* - 1$ where $\ell_*$ is the minimum of all of the labels in the tree. For another vertex $v$ in the tree with label $\ell$, the distance between $v$ and $v_*$ in the quadrangulation is given by $\ell - \ell_* + 1$. One can therefore extract from this that the diameter of a typical random quadrangulation with $n$ faces is of order $n^{1/4}$ because the displacement of the encoding walk for the associated tree will be of order $n^{1/2}$ so the maximum label (in absolute value) will be of order $n^{1/4}$.

Independently of the motivation described in the second paragraph of Section 4.1, it is very interesting to study the large-scale behavior of these RPM as in the scaling limit the resulting object can be thought of as a continuum surface chosen uniformly at random in the same way that Brownian motion can be thought of as a continuous curve chosen uniformly at random. It was proved by Chassaing and Schaeffer [19] that the well-labeled tree structure converges in the limit to a continuous object called the *Brownian snake*. The Brownian snake is a continuous analog of a random well-labeled tree where the tree part is given by a *continuum random tree* (CRT) [3] $\mathcal{T}$ and, given $\mathcal{T}$, the labels are described by a Brownian motion indexed by $\mathcal{T}$. This means that the labels starting from the root of $\mathcal{T}$ evolve as a standard Brownian motion as one goes up any fixed branch of the tree and these Brownian motions become independent whenever branches separate. The name *Brownian map* was coined by Marckert and Mokkadem in [88] and this is the continuous object which describes the scaling limit of the metric space (rather than encoding) structure of such a RPM.

There are many works which are aimed at establishing the convergence of the metric measure space structure $(M_n, d_n, \mu_n)$ of such a RPM towards the Brownian map. The topology for taking this limit comes from the *Gromov-Hausdorff-Prokhorov* distance, which is a metric on the space of compact metric spaces equipped with a measure. As explained above, when the underlying map has $n$ faces the correct normalization factor for the distance on the map is $n^{-1/4}$. The tightness of the law of $(M_n, n^{-1/4} d_n, n^{-1} \mu_n)$ was proved in [79]. It took a number of years before the subsequential convergence was promoted to actual convergence and a number of important results were proved in the intervening period. For example, in [84, 90] it was shown that every subsequential limit is a topological sphere and in [79] that every subsequential limit has Hausdorff dimension 4. A number of important properties of geodesics were studied in [80], in particular the so-called *confluence of geodesics phenomenon* which states that any pair of geodesics towards a "typical" point eventually agree. The convergence of the actual metric-measure space struc-

ture was proved in independent works of Le Gall [81] and Miermont [91]. The latter work focuses on the case of triangulations while the former proves in addition the convergence in the case of $p$-angulations for $p = 3$ and $p \geq 4$ even. The convergence for $p$-angulations with $p \geq 3$ odd was proved by [1]. Scaling limits have subsequently been proved for a number of other topologies (see, e.g., [15, 16, 23, 43]). In order to distinguish the different topologies, the Brownian map is now called the *Brownian sphere* and the other possible topologies make up the family of *Brownian surfaces*. We emphasize that all of these scaling limit results lead to an abstract metric measure space but do not concern a canonical way of drawing the limit in the plane.

### 4.3 Random planar maps with extra structure

For the reasons mentioned in the second paragraph of Section 4.1, it is interesting to study RPM equipped with the extra structure of a statistical mechanics model. In this case, one picks a *pair* $(M, X)$ where $M$ is a planar map and $X$ is a distinguished structure on the map. This leads to a so-called *decorated* RPM. It is important to choose the law on RPM so that the resulting object has the correct Markov properties. In particular, one would like to have a simple description of the conditional law of the RPM when one explores the interfaces of $X$ in a Markovian way. The correct way to do this is to bias the uniform distribution on maps by the partition function of the associated statistical mechanics model. For example, in the case of a spanning tree decorated planar map this corresponds to choosing $(M, X)$ uniformly at random from the set of map-spanning tree pairs so that the marginal law of $M$ is biased by the number of spanning trees that it contains. This has the effect of changing the macroscopic behavior of $M$ quite significantly in comparison to, say, the RPM described in Section 4.2 and the scaling limit is not described by a Brownian surface.

One often studies decorated RPM using bijective techniques as in the case of uniform RPM and these bijections typically encode the decorated RPM in terms of trees as before. The key difference is that for uniform RPM the well-labeled tree structure serves to naturally encode the metric structure of the map whereas for decorated RPM the tree structure jointly encodes the map and the statistical mechanics model but the graph metric is not easily accessible. In the case of tree-decorated RPM, the bijection is due to Mullin [106] and it is remarkably simple. The Mullin bijection was extended to the case of a decorated RPM with an instance of the FK model in [122] and bijections in this spirit have been constructed for a number of other models in the works [42, 67, 85]. In each of these works, scaling limit results are proved for the encoding structure of the underlying map (in analogy with [19]) and the scaling limit is described by a coupled pair of CRTs which in turn can be described by a correlated Brownian motion.

It is expected that the convergence also holds in the Gromov-Hausdorff-Prokhorov topology, but this has not yet been proved for these models except in one case. Namely, one can consider so-called RPM with *large faces*. This refers to a RPM model where the face degrees are random rather than fixed and the degree has a heavy tail. This model was first considered in [83] as a toy model for the result of considering a loop model on a RPM (e.g., the Ising model) and then looking at the resulting metric after one removes the parts of the map which are surrounded by one of the loops.

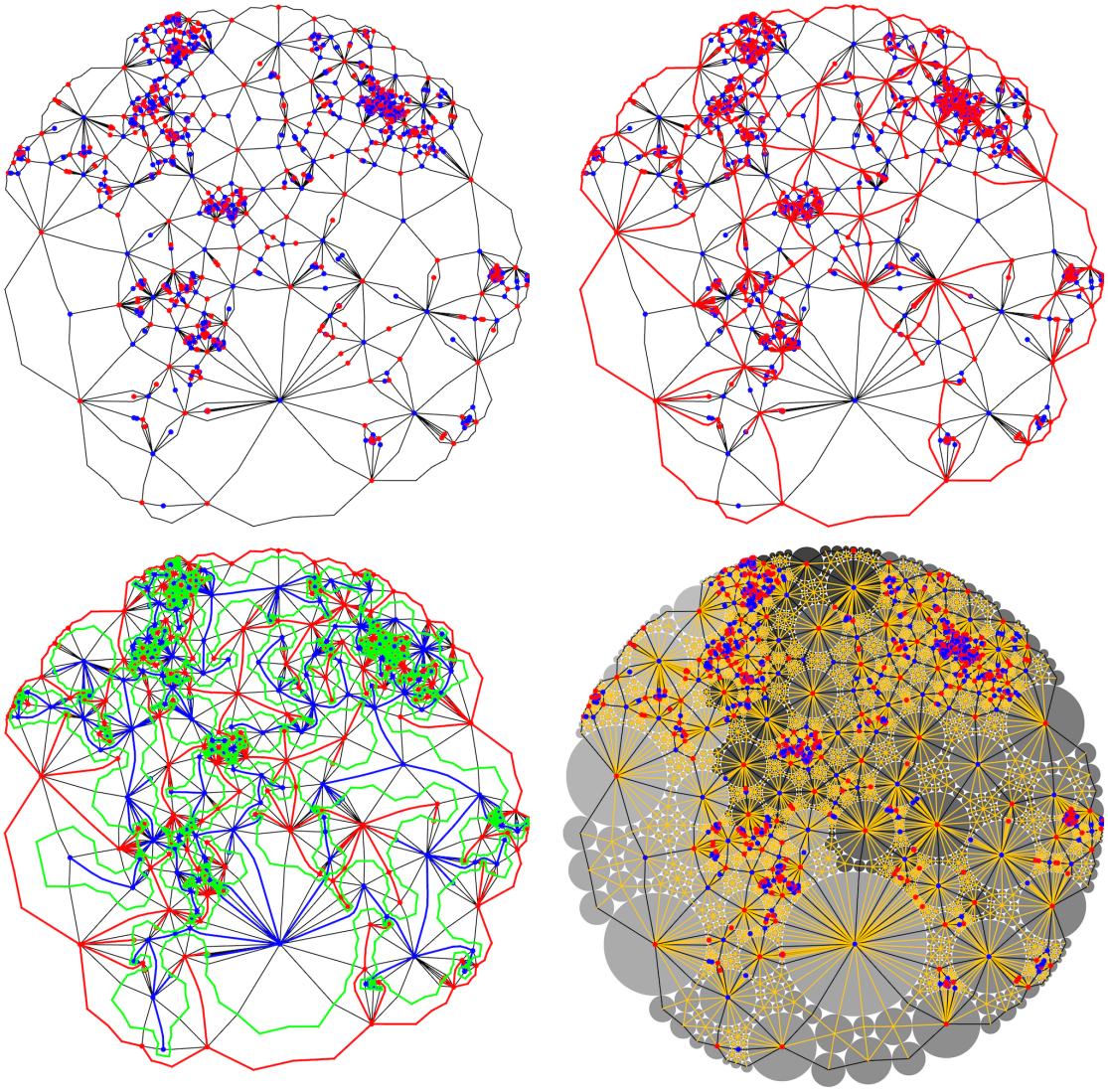

FIGURE 8 – **Top left :** A random quadrangulation of the disk sampled using the Mullin bijection [106] (quadrilaterals on the boundary are divided into triangles). The map is bipartite and the two classes are colored red and blue. **Top right :** A distinguished spanning tree (red) consisting of diagonals of quadrilaterals with wired boundary conditions. **Bottom left :** The spanning tree (red) together with its dual (blue) and the Peano curve which snakes between them (green). **Bottom right :** The embedding was constructed by subdividing each quadrilateral into triangles (yellow edges) and then computing the circle packing of the resulting triangulation using [128]. (Circle packing is a discrete form of conformal mapping [113].)

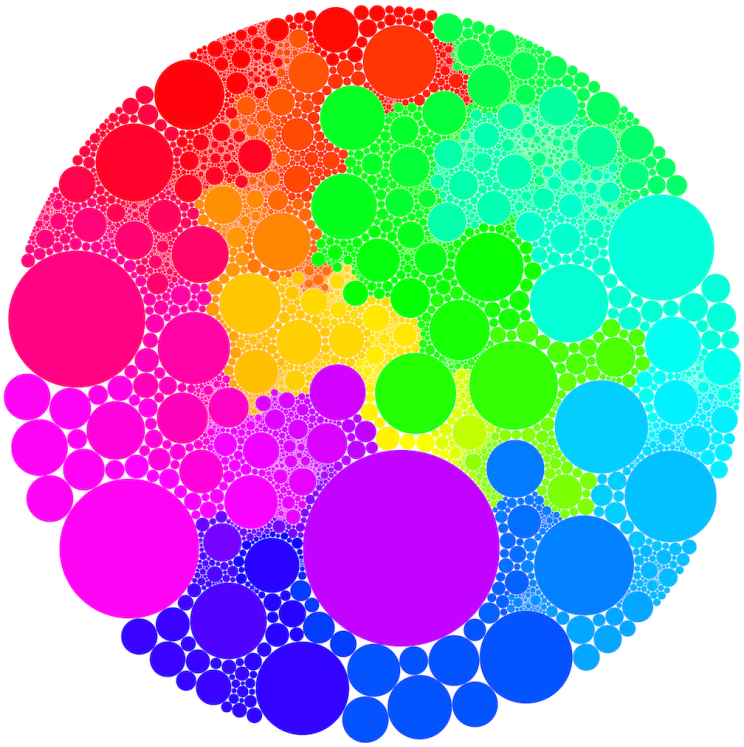

Figure 9 – Continuation of Figure 8. Circles are colored according to the order in which they are visited by the Peano curve.

The tightness of the associated metric space was proved in [83] and forthcoming work [24] will prove the full convergence to the so-called *stable maps*.

We note that it is possible to enumerate planar maps using various types of random matrices (see [2, 36] and the references therein for an overview). For this reason, these models are sometimes referred to as *matrix models*.

## 5 Liouville quantum gravity

### 5.1 Definition

The Liouville quantum gravity (LQG) surfaces are in a certain sense the canonical model for a random two-dimensional Riemannian manifold. LQG was introduced by Polyakov in the 1980s in the context of string theory [108, 109]. It is defined in terms of the metric tensor

$$e^{\gamma h(z)}(dx^2 + dy^2) \tag{11}$$

where $h$ is an instance of (some form of) the GFF on a planar domain $D$, $\gamma \in (0, 2]$ is a parameter, and $dx^2 + dy^2$ denotes the Euclidean metric on $D$. The parameter $\gamma$ determines the degree to which the resulting surface is perturbed from a Euclidean geometry : when $\gamma = 0$ one simply has a Euclidean metric but as $\gamma$ increases to 2 an LQG surface becomes increasingly fractal. Since the GFF is not a function, the expression (11) does not make literal sense and requires interpretation. The volume form associated with (11) was first constructed in [52] for $\gamma \in (0, \sqrt{2})$. This

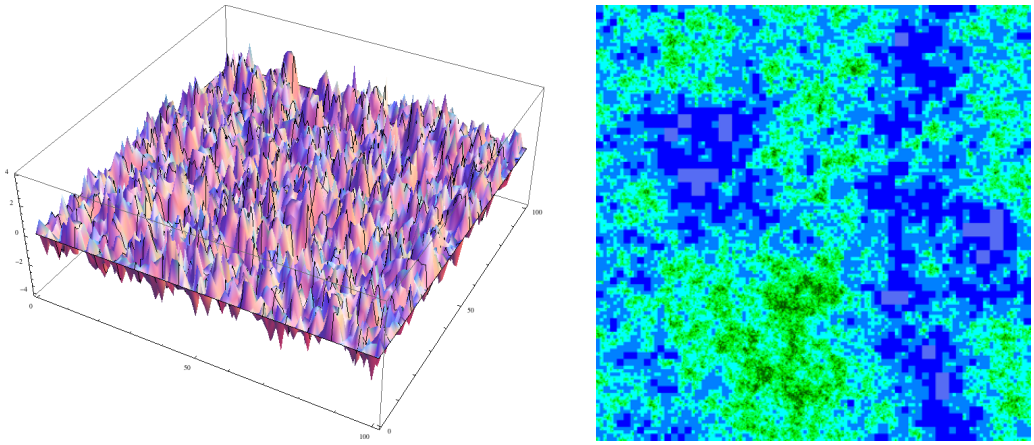

FIGURE 10 – **Left :** Simulation of the GFF on lattice, an approximation of the continuum GFF. **Right :** Simulation of the LQG measure with $\gamma = 1$. Each square shown has approximately the same size (as measured using LQG area) but very different Euclidean sizes.

parameter range is special because it corresponds to what is now called the $L^2$-regime since in this case the measure that the resulting volume form assigns to any fixed compact set has a finite second moment. It can be constructed for the full range $\gamma \in (0,2)$ using Kahane's theory of Gaussian multiplicative chaos [59]. It was also constructed in [35] by replacing $h$ with the function $h_\epsilon(z)$ which for $z \in D$ and $\epsilon > 0$ gives the average of $h$ on $\partial B(z,\epsilon)$ and then showing that the limit

$$\epsilon^{\gamma^2/2} e^{\gamma h_\epsilon(z)} dxdy \quad \text{as} \quad \epsilon \to 0 \tag{12}$$

exists where $dxdy$ denotes Lebesgue measure. The normalization factor $\epsilon^{\gamma^2/2}$ in (12) is necessary in order to get a non-trivial limit. The form of the normalization can be derived because for a GFF $h$ we have that $\mathrm{var}(h_\epsilon(z)) = \log \epsilon^{-1} + O(1)$.

In the case that $h$ has free boundary conditions and $L$ is a linear segment of $\partial D$, it is also possible to define a boundary length measure associated with $h$ on $L$. For $z \in L$, we set $h_\epsilon(z)$ to be the average of $h$ on $D \cap \partial B(z,\epsilon)$ and then the boundary length measure is defined as the limit

$$\epsilon^{\gamma^2/4} e^{\gamma h_\epsilon(z)/2} dx \quad \text{as} \quad \epsilon \to 0 \tag{13}$$

where $dx$ denotes Lebesgue measure on $L$. The form of the normalization can be derived because in the case of free boundary conditions on $L$ we have that $\mathrm{var}(h_\epsilon(x)) = 2\log \epsilon^{-1} + O(1)$ for $x \in L$.

The construction in the critical case that $\gamma = 2$ has some extra subtleties since if one normalizes by $\epsilon^2$ in (12) then the limiting measure vanishes (even though the mean of the approximations does not). To get a non-trivial limit in this case, one has to use instead the normalization $\epsilon^2 (\log \epsilon^{-1})^{1/2}$. One has to introduce a similar correction to (13) in order to define the critical boundary length measure. The critical measure was first constructed in [33, 34] and it was shown in [8] to be the limit as $\gamma \uparrow 2$ of the subcritical LQG area measures.

We will discuss later the construction of the *metric space* structure associated with (11) (which is what allows one to think of an LQG surface as a metric space

homeomorphic to a planar domain rather than just a random measure on a planar domain).

One way that the fact that the GFF is a distribution and not a function is reflected in the theory of LQG is that the dimensions of sets computed using LQG are not the same as their dimension computed using the Euclidean metric. For sets $X$ which are deterministic or more generally independent of $h$, the famous *KPZ formula* [68] relates the dimension of $X$ computed using LQG to its Euclidean dimension and is given by

$$x = \frac{\gamma^2}{4}\Delta^2 + \left(1 - \frac{\gamma^2}{4}\right)\Delta. \tag{14}$$

In (14), $x$ (resp. $\Delta$) describes the Euclidean (resp. quantum) scaling exponent. It is non-trivial to give a precise mathematical meaning to (14) as (11) requires interpretation. In particular, one has to specify the notion of dimension that one is using. The first rigorous versions of (14) were proved in [12, 35, 111]. For example, in [35] (14) is interpreted as meaning that the Lebesgue measure of the $\epsilon$-neighborhood of $X$ behaves like $\epsilon^{2x}$ as $\epsilon \to 0$ and the quantum measure of the quantum-$\delta$-neighborhood behaves like $\delta^{\Delta}$ as $\delta \to 0$. Here, the quantum-$\delta$-neighborhood is the union of all *Euclidean* balls which have quantum area $\delta$ and intersect $X$. Since [12, 35, 111], a number of other works have established other rigorous versions of (14), some of which we will describe below, and make use of other notions of dimension and scaling exponents.

Soon after the introduction of LQG and the discovery of the KPZ formula, it was conjectured that LQG describes the continuous limit of RPM. This was made on the basis that critical exponents for models from statistical mechanics on RPM transform to the corresponding exponent on a Euclidean lattice according to the KPZ formula. In [110], Polyakov himself made the following comment about this conjecture (recall that matrix models refer to RPMs) :

> *A few years before this work Kazakov and David suggested that the discrete version of 2D gravity can be described by the various matrix models. It was hard to be certain that these models really have a continuous limit described by the Liouville theory, there were no proofs of this conjecture. To our surprise we found that the anomalous dimensions coming from our theory coincide with the ones computed from the matrix model. That left no doubts that in the case of the minimal models the Liouville description is equivalent to the matrix one. This relation received a lot of attention.*

### 5.2 Relationship with SLE

There are many deep connections between SLE and LQG. The first rigorous result relating SLE and LQG is the so-called *quantum zipper theorem* due to Sheffield [121]. The aim of [121] is to use the ansatz that SLE and LQG jointly describe the scaling limit of decorated RPM where the SLE curve gives the scaling limit of the interfaces of the loop model on the RPM as a guide for how SLE and LQG should be related in the continuum. The main result of [121] is concerned with making sense of the operation of gluing together two independent LQG surfaces with boundary and showing that the interface between the two surfaces is an SLE curve. This serves as a continuous analog of the operation of gluing together independently sampled

RPMs with boundary along their boundaries by identifying edges. This operation is particularly natural because the interface between two (properly chosen) RPMs glued together along their boundaries has the interpretation of being one of the interfaces from a statistical mechanics model on a RPM (it is the reverse of starting with a RPM with a statistical mechanics model and then dividing the map into pieces by cutting along an interface). The results from [121] are the starting point for a large number of works which serve to develop the relationship between SLE and LQG, use it make connections between RPMs, and also to prove a number of new results about SLE and related processes.

The way that the gluing of LQG surfaces is defined in [121] is using *conformal welding* and this indeed leads to the fourth construction of SLE mentioned in Section 2.3. Let us review the definition of a conformal welding in the context of gluing together two copies of the unit disk $\mathbf{D}_1$, $\mathbf{D}_2$. Suppose that $\phi\colon \partial\mathbf{D}_1 \to \partial\mathbf{D}_2$ is a homeomorphism. Then a *conformal welding with welding homeomorphism* $\phi$ consists of a simple loop $\eta$ on $\mathbf{S}^2$ together with a pair of conformal maps $\psi_1, \psi_2$ which take $\mathbf{D}_1, \mathbf{D}_2$ to the left and right sides of $\mathbf{S}^2 \setminus \eta$ with the property that $\psi_2^{-1} \circ \psi_1|_{\partial\mathbf{D}_1} = \phi$ ; $\eta$ is referred to as the *welding interface*. One can more generally consider the conformal welding of $\mathbf{D}_1$, $\mathbf{D}_2$ where only an interval of each of their boundaries are identified and the result will be a disk together with a simple curve on it connecting two boundary points. It is not obvious that a conformal welding exists for a given welding homeomorphism $\phi$ and if it exists it is not obvious that it is unique.

In the setting of [121], the main result is focused on welding together LQG surfaces (so called *quantum wedges*) which are "half-plane like" meaning that they have a distinguished origin and $\infty$ where compact neighborhoods of the origin have a finite amount of LQG area and neighborhoods of $\infty$ all have an infinite amount of LQG area. Moreover, the welding operation considered involves identifying the positive boundary ray of one surface with the negative boundary ray of the other surface using LQG length. The quantum wedge considered describes the local behavior of an LQG surface with boundary near a typical point chosen from the quantum boundary length measure. This particular setting is the one which is considered as it is the one in which the welding interface is exactly a chordal $\mathrm{SLE}_\kappa$ which is *independent* of the resulting LQG surface ; variants of this setup yield other types of SLE curves. In order for the welding operation to be defined, one needs that $\gamma \in (0,2)$ and $\kappa = \gamma^2$. This result also allows one to make sense of the quantum length of an $\mathrm{SLE}_\kappa$ curve. (We remark that other works have studied random conformal weldings, for example [9], which considers the random conformal welding associated with an LQG surface and a Euclidean disk.)

Once one shows that a conformal welding associated with a given welding homeomorphism exists, establishing the uniqueness amounts to showing that the welding interface is *conformally removable*. Recall that $K \subseteq \mathbf{C}$ is said to be conformally removable if whenever $\varphi\colon \mathbf{C} \to \mathbf{C}$ is a homeomorphism which is conformal off $K$ then it is conformal everywhere. One often establishes conformal removability by invoking one of the conditions from [58]. In the case of $\mathrm{SLE}_\kappa$ for $\kappa \in (0,4)$, one can use that boundaries of Hölder domains are conformally removable [58] and that the complementary components of an $\mathrm{SLE}_\kappa$ curve for $\kappa \neq 4$ are always Hölder domains [114].

The construction from [121] was extended to include the $\mathrm{SLE}_{\kappa'}$ processes for $\kappa' > 4$ in [32] (see also [53] for the existence of the critical welding and [61] for

the uniqueness). In the case that $\kappa' \in (4,8)$, the surfaces which are to the left and right of an $\mathrm{SLE}_{\kappa'}$ process do not consist of a single component but rather an entire trees of surfaces. For $\kappa' > 4$, the $\mathrm{SLE}_{\kappa'}$ is space-filling and so we can represent it as a mating of trees. Uniqueness results in these settings were proved in [32]; see also [62] for a removability result for $\kappa' \in (4,8)$. See just below for more on tree mating constructions.

### 5.3 Mating of trees representation

The *mating of trees representation* of LQG [32] is a continuous analog of the tree bijections for planar maps mentioned in Section 4.3 where the LQG surface plays the role of the underlying RPM and the role of the extra structure on the RPM is played by an SLE curve which is independent of the LQG surface. It serves to provide a framework for proving scaling limit results of RPM towards LQG surfaces decorated with SLE curves and also provides another tool for proving results about SLE itself.

Let us now describe in more detail one of the *mating of trees* theorems proved in [32]. For what we will describe it is convenient to consider the case in which we are working with the whole-plane topology. The underlying quantum surface in this case is called a *quantum cone*, which is an infinite volume LQG surface with the topology of $\mathbf{C}$ with marked points at the origin and at $\infty$. Compact neighborhoods of the origin a.s. have finite LQG area and neighborhoods of $\infty$ have infinite LQG area. One way to think about a quantum cone is that it describes the local behavior of an LQG surface (i.e., after "zooming in") at a point which is chosen from the LQG measure.

Fix $\gamma \in (0,2)$, $\kappa = \gamma^2$, and $\kappa' = 16/\gamma^2$. The SLE process $\eta'$ that one considers is a so-called "space-filling $\mathrm{SLE}_{\kappa'}$ in $\mathbf{C}$ from $\infty$ to $\infty$". The most direct way to construct this space-filling $\mathrm{SLE}_{\kappa'}$ process is by using a whole-plane GFF $h^{\mathrm{IG}}$ which is independent of the quantum cone. The field $h^{\mathrm{IG}}$ will serve to encode an independent "imaginary geometry", which is the reason for the notation. It is not possible for a whole-plane GFF to have well-defined values, so it is in fact considered modulo a global multiple of $2\pi\chi$ where $\chi$ is as in (9). For each $z \in \mathbf{C}$, we let $\eta_z^L$ be the flow line of $h^{\mathrm{IG}}$ starting from $z$ with angle $\pi/2$. For $z, w \in \mathbf{C}$ distinct, as we explained earlier, the flow lines $\eta_z^L$, $\eta_z^L$ will a.s. merge into each other. Then we say that $z$ comes before $w$ if $\eta_z^L$ merges into $\eta_w^L$ on its left side. Suppose that $(z_n)$ is a countable dense set in $\mathbf{C}$. Then we can use this procedure to define an ordering of the $(z_n)$. It is proved in [97] that there exists a continuous curve $\eta'$ which visits the $(z_n)$ according to this order and this is the space-filling $\mathrm{SLE}_{\kappa'}$ in $\mathbf{C}$ from $\infty$ to $\infty$. One should think of the $\eta_z^L$ as branches in a space-filling tree and one can likewise define a space-filling dual tree by considering the family of flow lines $\eta_z^R$ starting from each $z \in \mathbf{C}$ with angle $-\pi/2$. Then $\eta'$ is the associated Peano curve which snakes between these two trees. In the case that $\kappa' \geq 8$, this process is characterized by the property that for each $t \in \mathbf{R}$ the conditional law of $\eta'|_{[t,\infty)}$ given $\eta'|_{(-\infty,t]}$ is that of an $\mathrm{SLE}_{\kappa'}$ in $\mathbf{C} \setminus \eta'((-\infty,t])$ from $\eta'(t)$ to $\infty$. In the case that $\kappa' \in (4,8)$, there are a countable number of components of $\mathbf{C} \setminus \eta'((-\infty,t])$ and the characterization is that in each of these components the curve is an $\mathrm{SLE}_{\kappa'}$ curve starting from the last point on the component boundary visited by $\eta'|_{(-\infty,t]}$ and targeted at the first point on the component boundary visited by $\eta'|_{(-\infty,t]}$.

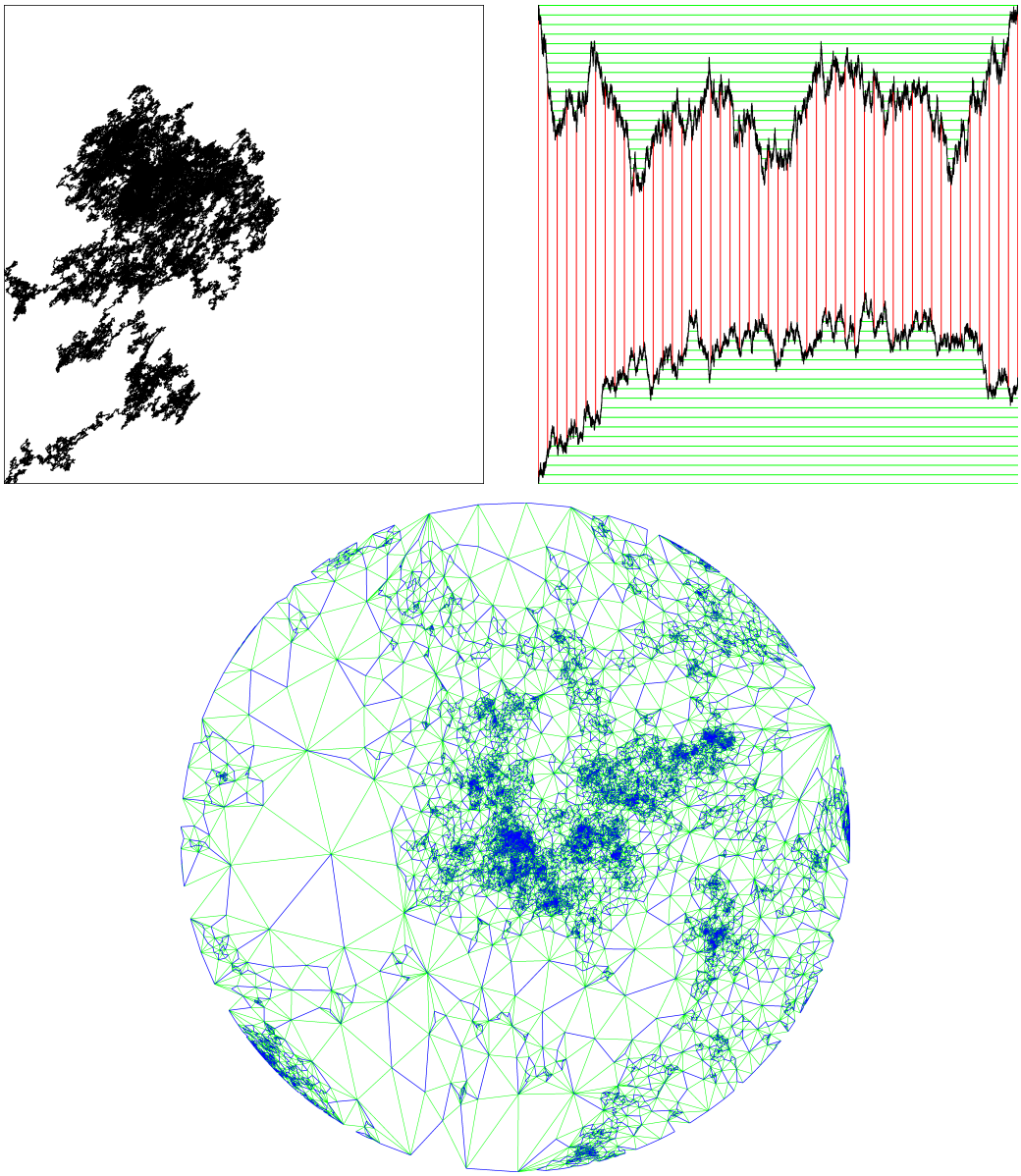

FIGURE 11 – Discrete approximation of the mating of trees representation of LQG. **Top left :** A correlated Brownian motion $(X, Y)$ starting from $(0, 0)$ and conditioned to exit $\mathbf{R}_+^2$ at $(0, 1)$ for the first time at time 1. **Top right :** Shown are the graphs of $C - X$ and $Y$ with $C > 0$ large enough so they are disjoint. Identifying the points which lie on horizontal chords either below the graph of $Y$ or above the graph of $C - X$ yields a pair of trees which are glued together by identifying points which lie on vertical chords between the two graphs. **Bottom :** The Tutte embedding of a discrete approximation of this equivalence relation (green) together with the Peano curve snaking between the two trees (blue).

In order to give the space-filling tree the structure of a (non-compact) $\mathbf{R}$-tree it is necessary for each of the branches to have an associated length measure. This measure is given by the $\gamma$-LQG boundary length measure. In order to identify the law of the resulting $\mathbf{R}$-trees in terms of their contour functions, is also important for the associated Peano curve $\eta'$ to have a time parameterization. The correct choice

corresponds to the $\gamma$-LQG area measure. The first "mating of trees" theorem is that with these choices of time parameterization, the associated contour functions $(X, Y)$ evolve as a two-dimensional two-sided Brownian motion with $X_0 = Y_0 = 0$ and (up to a deterministic linear reparameterization of time)

$$\mathrm{var}(X_t) = |t|, \quad \mathrm{var}(Y_t) = |t|, \quad \text{and} \quad \mathrm{cov}(X_t, Y_t) = -\cos\left(\frac{4\pi}{\kappa'}\right)|t| \quad \text{for} \quad t \in \mathbf{R}.$$

(The covariance $\mathrm{cov}(X_t, Y_t)$ was identified in [32] for $\kappa' \in (4, 8]$ and in [40] for $\kappa' > 8$.) Moreover, it is shown in [32] that it is possible to recover the SLE-decorated LQG surface, up to rotation, as a measurable function of $(X, Y)$. Other types of LQG surfaces can also be described in terms of mating of trees constructions. In particular, for finite volume surfaces such as disks or spheres the process $(X, Y)$ is replaced with a two-dimensional two-sided Brownian motion "conditioned" to be in the quadrant $\mathbf{R}^2_+$ (see the top left of Figure 11 for a numerical simulation in the case of the disk topology).

The aforementioned measurable function constructed in [32] is non-explicit. An explicit embedding was later constructed in [49] by associating with $(X, Y)$ a model of a RPM (the so-called "mated-CRT map") and then showing that the Tutte embedding of this map converges in the scaling limit to the embedding from [32] using an invariance principle for random walks in scale-free environments [50]. See Figure 11 for a numerical simulation.

The work [32] also establishes a number of other welding results for SLE processes and it is explained in [32, Appendix B] how one can use these welding results together with the KPZ formula (14) to derive many of the critical exponents which are associated with SLE and models which converge towards it. See also [39], which proves a version of the KPZ formula but formulated in terms of the encoding Brownian motion using the mating of trees theorem. It is also possible to derive new exponents for SLE and related processes using their encodings in terms of Brownian motions or more generally Lévy processes [103, 104].

## 6 Liouville quantum gravity metric

Recall from Section 5 that the expression (11) defining LQG requires interpretation and this was previously accomplished for the volume form and the boundary length measure. In order to think of an LQG surface as an actual surface, it is necessary to associate with it a *metric*, i.e., a two-point distance function. This is also desirable in order to relate LQG to RPM as the latter are graphs which can be encoded in terms of their associated metric space structure. The construction of the LQG metric was first accomplished in the case that $\gamma = \sqrt{8/3}$ in [99, 101, 102] and building further on [100] the equivalence of $\sqrt{8/3}$-LQG with the Brownian sphere is proved. The existence of the metric for $\gamma \in (0, 2)$ was later shown in [27, 46]. We will review the former in Section 6.1 and the latter in Section 6.2.

### 6.1 The case $\gamma = \sqrt{8/3}$

The value $\gamma = \sqrt{8/3}$ is special because the natural statistical mechanics models to put on a uniform RPM are percolation and the SAW. This can be seen in the case

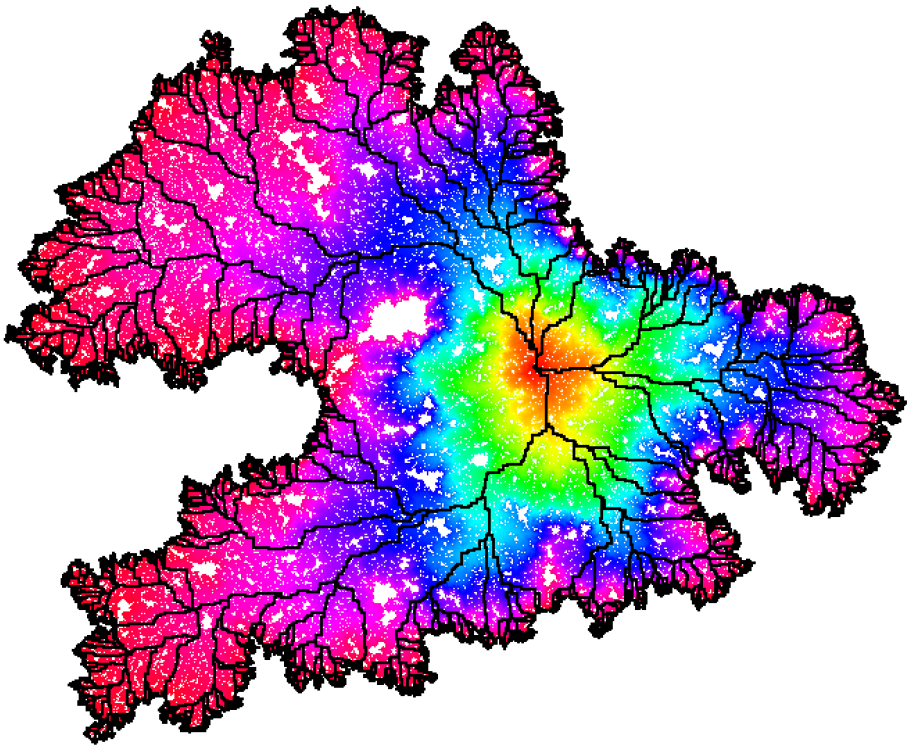

FIGURE 12 – A metric ball in $\sqrt{8/3}$-LQG together with geodesics from the boundary back to the center.

of the percolation model because in the case of, e.g., site percolation the partition function only depends on the number of vertices on the map so biasing by the associated partition function does not change the law of the map. On the other hand, a SAW-decorated RPM can be constructed by sampling two independent uniform RPM with the topology of the disk and the same boundary length and then gluing them together along their boundary ; the resulting interface is the SAW. Since the percolation model (resp. SAW) is related to $\mathrm{SLE}_6$ (resp. $\mathrm{SLE}_{8/3}$), the relationship $\gamma^2 = \kappa$ for $\kappa \in (0,4]$ or $\gamma^2 = 16/\kappa'$ for $\kappa' > 4$ yields that $\gamma = \sqrt{8/3}$ arises in each of these cases. This is one way of arriving at the conjecture that $\sqrt{8/3}$-LQG should be equivalent to the scaling limit of uniform RPM, i.e., the Brownian surfaces. Since a Brownian surface is a random metric measure space and $\sqrt{8/3}$-LQG (prior to having associated with it a metric space structure) is a random measure on a planar domain, one has to be careful in formulating a conjecture of the equivalence of objects of these two types. One way of going about this is to associate $\sqrt{8/3}$-LQG a metric space structure and then to conjecture that the resulting metric measure space has the same law as that of a Brownian surface. In making such a conjecture, one also has to specify the correct law on GFF-like distributions and it is different depending on the topology of the Brownian surface in question. In the case of the sphere, this corresponds to the $\sqrt{8/3}$-LQG sphere [32] (see also [25] for another approach to defining LQG on the sphere and [7] for a proof of their equivalence).

The construction of the metric in [99, 101, 102] is indirect and is based on a process called *quantum Loewner evolution* (QLE), which was previously introduced

in [96]. The idea of the construction is to try to make sense of a version of *first passage percolation* (FPP) on a $\sqrt{8/3}$-LQG surface. Recall that FPP on a graph $G = (V, E)$ (where every vertex has finite degree to avoid pathologies) starting from $x \in V$ is the growing family of clusters $C_n$ with $C_0 = \{x\}$ which are recursively constructed as follows. For each $n$, we let $C_{n+1}$ be given by $C_n \cup \{y\}$ where $y \in V$ is chosen uniformly at random from those $z \in V \setminus C_n$ for which there exists $w \in C_n$ with $\{z, w\} \in E$. That is, $C_{n+1}$ is formed from $C_n$ by adding to it a uniformly chosen element from the boundary of $C_n$. The FPP model is particularly convenient to consider on uniform RPM because as one grows an FPP cluster the conditional law of the unexplored regions of the map are given by independent uniform RPMs given their boundary lengths. The continuum version of FPP corresponding to QLE is constructed by replacing the RPM with a $\sqrt{8/3}$-LQG surface and the vertices added at each stage with chunks of $\mathrm{SLE}_6$ curves and then taking a limit as the size of the chunks tends to 0. The theory developed in [32] and extended in [98] allows one to see that, just like in the case of uniform RPMs, the conditional law of the unexplored surface at each stage is given by independent $\sqrt{8/3}$-LQG surfaces given their boundary lengths.

The aim of [99] is to show that the growth process defined by QLE corresponds to the balls in a metric space. This is a non-trivial statement because it is not obvious that the time for the growth process starting from $x$ to reach $y$ is equal to the time for the growth process starting from $y$ to reach $x$. The main result of [99] is that this symmetry holds and this leads to the construction of a metric which is defined on a countable dense subset of the $\sqrt{8/3}$-LQG sphere. It is then shown in [101] is that this metric extends continuously to the entire $\sqrt{8/3}$-LQG sphere, is Hölder continuous with respect to the Euclidean metric, and the resulting metric space satisfies the axiomatic characterization of the Brownian sphere given in [100] hence has the same law as the Brownian sphere.

The construction of the metric for $\sqrt{8/3}$-LQG and the proof of its equivalence with the Brownian sphere made it possible to show the joint convergence of statistical mechanics models on uniform RPM to SLE curves on $\sqrt{8/3}$-LQG with respect to the Gromov-Hausdorff-Prokhorov-uniform (GHPU) topology, which is a generalization of the Gromov-Hausdorff-Prokhorov topology where one keeps track of either a distinguished curve or a finite family of curves. Such convergence was proved for the SAW on RPM to $\mathrm{SLE}_{8/3}$ on $\sqrt{8/3}$-LQG in [45] and for the percolation model on RPM to $\mathrm{SLE}_6$ on $\sqrt{8/3}$-LQG in [47].

Following [99, 101], we have that the $\sqrt{8/3}$-LQG sphere has the structure of the Brownian sphere but it also contains the extra structure of an embedding in the plane (*a priori* the Brownian sphere does not come with this because it is only a metric measure space). It is then shown in [102] that given just the metric measure space structure of the $\sqrt{8/3}$-LQG sphere (i.e., the Brownian sphere) it is possible to recover in a measurable way its embedding into the plane, which implies that the Brownian sphere comes with a measurably defined embedding into the plane. This embedding, however, is proved to exist abstractly so is non-explicit. It is then natural to ask whether this embedding can be described in an explicit way and this question was addressed in the works [48, 50]. These works show that if one starts off with the Brownian sphere and then constructs a graph approximation by considering the Poisson-Voronoi tessellation then the associated Tutte embedding converges in

the limit to the embedding which is shown to exist abstractly in [102]. (Another approach to the embedding problem for uniform RPM was developed in [54] based on [47].)

### 6.2 The case $\gamma \in (0,2)$

The LQG metric for general values of $\gamma \in (0,2)$ was constructed in [27, 46] and the construction is based on an explicit approximation procedure. Namely, one lets

$$\xi = \frac{\gamma}{d(\gamma)} \quad \text{for each} \quad \gamma \in (0,2) \tag{15}$$

where $d(\gamma)$ denotes the "ball volume growth exponent" of $\gamma$-LQG. The value of $d(\gamma)$ is only known in the case $\gamma = \sqrt{8/3}$ due to the equivalence of $\sqrt{8/3}$-LQG with the Brownian sphere and in this case we have that $d(\sqrt{8/3}) = 4$. One then considers the so-called *Liouville first passage percolation* (LFPP) distance

$$\mathfrak{d}_\epsilon(x,y) = \inf_P \int_0^1 e^{\xi h_\epsilon(P(t))} |P'(t)| dt \tag{16}$$

where the infimum is over all paths $P$ defined on $[0,1]$ which connect $x$ and $y$ and $h_\epsilon$ denotes a certain regularization of the GFF. It is proved in [27] that if we let $\mathfrak{m}_\epsilon$ denote the median length of a crossing defined using (16) then the law of $(x,y) \mapsto \mathfrak{m}_\epsilon^{-1} \mathfrak{d}_\epsilon(x,y)$ is tight and that the subsequential limits define a non-trivial metric which is Hölder continuous with respect to the Euclidean metric. The work [46] then shows that the subsequential limits exist and are characterized by a certain list of axioms. The proof in [46] makes heavy use of the confluence of geodesics phenomenon for the $\gamma$-LQG metric established in [44]. In particular, since the $\sqrt{8/3}$-LQG metric previously constructed satisfies these axioms the two constructions give the same object for $\gamma = \sqrt{8/3}$.

Let us now explain why one uses the exponent $\xi$ in (16) in place of, say, $\gamma$. Suppose that $B_h(x,\epsilon)$ denotes a ball of radius $\epsilon$ with respect to the $\gamma$-LQG metric defined in terms of the field $h$. Then we have that $\mu_h(B_h(x,\epsilon)) \approx \epsilon^{d(\gamma)}$. Fix $C \in \mathbf{R}$. Then replacing $h$ with $h + C$ has the effect of multiplying $\gamma$-LQG areas by $e^{\gamma C}$ and $\gamma$-LQG distances by $e^{\xi C}$. We thus have on the one hand that

$$\mu_{h+C}(B_{h+C}(x,\epsilon)) \approx \epsilon^{d(\gamma)} \quad \text{as} \quad \epsilon \to 0$$

(since if $h$ is a GFF then so is $h + C$) and on the other hand that

$$\begin{aligned} \mu_{h+C}(B_{h+C}(x,\epsilon)) &= e^{\gamma C} \mu_h(B_h(x, e^{-\xi C}\epsilon)) \approx e^{\gamma C}(e^{-\xi C}\epsilon)^{d(\gamma)} \\ &= e^{(\gamma - \xi d(\gamma))C} \epsilon^{d(\gamma)} \quad \text{as} \quad \epsilon \to 0. \end{aligned}$$

Equating, we see that $\xi = \gamma/d(\gamma)$. As we mentioned earlier, $d(\gamma)$ hence $\xi$ is only known for $\gamma = \sqrt{8/3}$.

Tightness of approximations as in (16) the existence of the limit in the *super-critical regime* ($\xi > 2/d(2)$) was established in [28, 29]. In this case, the resulting metric space is *not* homeomorphic to Euclidean space.

## 7 Liouville conformal field theory

Parallel to the development of the connections between SLE and LQG has been the mathematically rigorous construction of *Liouville conformal field theory* (LCFT). This started with the construction of Liouville quantum gravity on the sphere [25] and later in the case of other topologies [38, 55]. (We note that there is another approach to constructing LQG on the disk and sphere developed in [32] and the two approaches were proved to be equivalent in [7, 18].) The so-called DOZZ formula describes the 3-point correlation function for LCFT on the sphere and was rigorously proved in [69] and the conformal bootstrap gives an inductive procedure for obtaining higher order correlation functions and was rigorously proved for LCFT in [37].

Several recent works have combined the results proved for LCFT, in particular the DOZZ formula, and for SLE on LQG in order to derive a number of new exponents and formulas for SLE and related processes. Some notable examples include the derivation of the moments the conformal derivative for the $\mathrm{SLE}_\kappa(\rho)$ processes [5], the electrical thickness formula for $\mathrm{CLE}_\kappa$ loops [6], and the backbone exponent $\mathrm{CLE}_\kappa$ (in particular for critical percolation) [107].

## Références


[1] L. Addario-Berry and M. Albenque. Convergence of odd-angulations via symmetrization of labeled trees. *arXiv e-prints*, page arXiv :1904.04786, Apr. 2019.

[2] G. Akemann, J. Baik, and P. Di Francesco, editors. *The Oxford handbook of random matrix theory*. Oxford University Press, Oxford, 2015. Paperback edition of the 2011 original [ MR2920518].

[3] D. Aldous. The continuum random tree. I. *Ann. Probab.*, 19(1) :1–28, 1991.

[4] V. Ambrosio and J. Miller. A continuous proof of the existence of the $\mathrm{SLE}_8$ curve. *arXiv e-prints*, page arXiv :2203.13805, Mar. 2022.

[5] M. Ang, N. Holden, and X. Sun. Integrability of SLE via conformal welding of random surfaces. *arXiv e-prints*, page arXiv :2104.09477, Apr. 2021.

[6] M. Ang and X. Sun. Integrability of the conformal loop ensemble. *arXiv e-prints*, page arXiv :2107.01788, July 2021.

[7] J. Aru, Y. Huang, and X. Sun. Two perspectives of the 2D unit area quantum sphere and their equivalence. *Comm. Math. Phys.*, 356(1) :261–283, 2017.

[8] J. Aru, E. Powell, and A. Sepúlveda. Critical Liouville measure as a limit of subcritical measures. *Electron. Commun. Probab.*, 24 :Paper No. 18, 16, 2019.

[9] K. Astala, P. Jones, A. Kupiainen, and E. Saksman. Random conformal weldings. *Acta Math.*, 207(2) :203–254, 2011.

[10] V. Beffara. The dimension of the SLE curves. *Ann. Probab.*, 36(4) :1421–1452, 2008.

[11] D. Beliaev and S. Smirnov. Harmonic measure and SLE. *Comm. Math. Phys.*, 290(2) :577–595, 2009.

[12] I. Benjamini and O. Schramm. KPZ in one dimensional random geometry of multiplicative cascades. *Comm. Math. Phys.*, 289(2) :653–662, 2009.

[13] S. Benoist and C. Hongler. The scaling limit of critical Ising interfaces is $CLE_3$. *Ann. Probab.*, 47(4) :2049–2086, 2019.

[14] N. Berestycki and J. Norris. *Lectures on Schramm-Loewner evolutions*. 2016.

[15] J. Bettinelli and G. Miermont. Compact Brownian surfaces I : Brownian disks. *Probab. Theory Related Fields*, 167(3-4) :555–614, 2017.

[16] J. Bettinelli and G. Miermont. Compact Brownian surfaces II. Orientable surfaces. *arXiv e-prints*, page arXiv :2212.12511, Dec. 2022.

[17] F. Camia and C. M. Newman. Critical percolation exploration path and $SLE_6$ : a proof of convergence. *Probab. Theory Related Fields*, 139(3-4) :473–519, 2007.

[18] B. Cerclé. Unit boundary length quantum disk : a study of two different perspectives and their equivalence. *ESAIM Probab. Stat.*, 25 :433–459, 2021.

[19] P. Chassaing and G. Schaeffer. Random planar lattices and integrated super-Brownian excursion. *Probab. Theory Related Fields*, 128(2) :161–212, 2004.

[20] D. Chelkak, H. Duminil-Copin, C. Hongler, A. Kemppainen, and S. Smirnov. Convergence of Ising interfaces to Schramm's SLE curves. *C. R. Math. Acad. Sci. Paris*, 352(2) :157–161, 2014.

[21] R. Cori and B. Vauquelin. Planar maps are well labeled trees. *Canadian J. Math.*, 33(5) :1023–1042, 1981.

[22] N. Curien. Peeling random planar maps. *Saint-Flour lecture notes*, 2019.

[23] N. Curien and J.-F. Le Gall. The Brownian plane. *J. Theoret. Probab.*, 27(4) :1249–1291, 2014.

[24] N. Curien, G. Miermont, and A. Riera. The scaling limit of random planar maps with large faces. 2023. In preparation.

[25] F. David, A. Kupiainen, R. Rhodes, and V. Vargas. Liouville quantum gravity on the Riemann sphere. *Comm. Math. Phys.*, 342(3) :869–907, 2016.

[26] L. de Branges. A proof of the Bieberbach conjecture. *Acta Math.*, 154(1-2) :137–152, 1985.

[27] J. Ding, J. Dubédat, A. Dunlap, and H. Falconet. Tightness of Liouville first passage percolation for $\gamma \in (0, 2)$. *Publ. Math. Inst. Hautes Études Sci.*, 132 :353–403, 2020.

[28] J. Ding and E. Gwynne. Tightness of supercritical Liouville first passage percolation. *J. Eur. Math. Soc. (JEMS)*, 25(10) :3833–3911, 2023.

[29] J. Ding and E. Gwynne. Uniqueness of the critical and supercritical Liouville quantum gravity metrics. *Proc. Lond. Math. Soc. (3)*, 126(1) :216–333, 2023.

[30] J. Dubédat. Duality of Schramm-Loewner evolutions. *Ann. Sci. Éc. Norm. Supér. (4)*, 42(5) :697–724, 2009.

[31] J. Dubédat. SLE and the free field : partition functions and couplings. *J. Amer. Math. Soc.*, 22(4) :995–1054, 2009.

[32] B. Duplantier, J. Miller, and S. Sheffield. Liouville quantum gravity as a mating of trees. *Astérisque*, (427) :viii+257, 2021.

[33] B. Duplantier, R. Rhodes, S. Sheffield, and V. Vargas. Critical Gaussian multiplicative chaos : convergence of the derivative martingale. *Ann. Probab.*, 42(5) :1769–1808, 2014.

[34] B. Duplantier, R. Rhodes, S. Sheffield, and V. Vargas. Renormalization of critical Gaussian multiplicative chaos and KPZ relation. *Comm. Math. Phys.*, 330(1) :283–330, 2014.

[35] B. Duplantier and S. Sheffield. Liouville quantum gravity and KPZ. *Invent. Math.*, 185(2) :333–393, 2011.

[36] B. Eynard. Formal matrix integrals and combinatorics of maps. In *Random matrices, random processes and integrable systems*, CRM Ser. Math. Phys., pages 415–442. Springer, New York, 2011.

[37] C. Guillarmou, A. Kupiainen, R. Rhodes, and V. Vargas. Conformal bootstrap in Liouville Theory. *arXiv e-prints*, page arXiv :2005.11530, May 2020.

[38] C. Guillarmou, R. Rhodes, and V. Vargas. Polyakov's formulation of $2d$ bosonic string theory. *Publ. Math. Inst. Hautes Études Sci.*, 130 :111–185, 2019.

[39] E. Gwynne, N. Holden, and J. Miller. An almost sure KPZ relation for SLE and Brownian motion. *Ann. Probab.*, 48(2) :527–573, 2020.

[40] E. Gwynne, N. Holden, J. Miller, and X. Sun. Brownian motion correlation in the peanosphere for $\kappa > 8$. *Ann. Inst. Henri Poincaré Probab. Stat.*, 53(4) :1866–1889, 2017.

[41] E. Gwynne, N. Holden, and X. Sun. Mating of trees for random planar maps and Liouville quantum gravity : a survey. In *Topics in statistical mechanics*, volume 59 of *Panor. Synthèses*, pages 41–120. Soc. Math. France, Paris, 2023.

[42] E. Gwynne, A. Kassel, J. Miller, and D. B. Wilson. Active spanning trees with bending energy on planar maps and SLE-decorated Liouville quantum gravity for $\kappa > 8$. *Comm. Math. Phys.*, 358(3) :1065–1115, 2018.

[43] E. Gwynne and J. Miller. Convergence of the free Boltzmann quadrangulation with simple boundary to the Brownian disk. *Ann. Inst. Henri Poincaré Probab. Stat.*, 55(1) :551–589, 2019.

[44] E. Gwynne and J. Miller. Confluence of geodesics in Liouville quantum gravity for $\gamma \in (0, 2)$. *Ann. Probab.*, 48(4) :1861–1901, 2020.

[45] E. Gwynne and J. Miller. Convergence of the self-avoiding walk on random quadrangulations to $\mathrm{SLE}_{8/3}$ on $\sqrt{8/3}$-Liouville quantum gravity. *Ann. Sci. Éc. Norm. Supér. (4)*, 54(2) :305–405, 2021.

[46] E. Gwynne and J. Miller. Existence and uniqueness of the Liouville quantum gravity metric for $\gamma \in (0, 2)$. *Invent. Math.*, 223(1) :213–333, 2021.

[47] E. Gwynne and J. Miller. Percolation on uniform quadrangulations and $\mathrm{SLE}_6$ on $\sqrt{8/3}$-Liouville quantum gravity. *Astérisque*, (429) :vii+242, 2021.

[48] E. Gwynne, J. Miller, and S. Sheffield. The Tutte embedding of the Poisson-Voronoi tessellation of the Brownian disk converges to $\sqrt{8/3}$-Liouville quantum gravity. *Comm. Math. Phys.*, 374(2) :735–784, 2020.

[49] E. Gwynne, J. Miller, and S. Sheffield. The Tutte embedding of the mated-CRT map converges to Liouville quantum gravity. *Ann. Probab.*, 49(4) :1677–1717, 2021.

[50] E. Gwynne, J. Miller, and S. Sheffield. An invariance principle for ergodic scale-free random environments. *Acta Math.*, 228(2) :303–384, 2022.

[51] E. Gwynne, J. Miller, and X. Sun. Almost sure multifractal spectrum of Schramm-Loewner evolution. *Duke Math. J.*, 167(6) :1099–1237, 2018.

[52] R. Hø egh Krohn. A general class of quantum fields without cut-offs in two space-time dimensions. *Comm. Math. Phys.*, 21 :244–255, 1971.

[53] N. Holden and E. Powell. Conformal welding for critical Liouville quantum gravity. *Ann. Inst. Henri Poincaré Probab. Stat.*, 57(3) :1229–1254, 2021.

[54] N. Holden and X. Sun. Convergence of uniform triangulations under the Cardy embedding. *Acta Math.*, 230(1) :93–203, 2023.

[55] Y. Huang, R. Rhodes, and V. Vargas. Liouville quantum gravity on the unit disk. *Ann. Inst. Henri Poincaré Probab. Stat.*, 54(3) :1694–1730, 2018.

[56] F. Johansson Viklund and G. F. Lawler. Optimal Hölder exponent for the SLE path. *Duke Math. J.*, 159(3) :351–383, 2011.

[57] F. Johansson Viklund and G. F. Lawler. Almost sure multifractal spectrum for the tip of an SLE curve. *Acta Math.*, 209(2) :265–322, 2012.

[58] P. W. Jones and S. K. Smirnov. Removability theorems for Sobolev functions and quasiconformal maps. *Ark. Mat.*, 38(2) :263–279, 2000.

[59] J.-P. Kahane. Sur le chaos multiplicatif. *Ann. Sci. Math. Québec*, 9(2) :105–150, 1985.

[60] K. Kavvadias, J. Miller, and L. Schoug. Regularity of the $\mathrm{SLE}_4$ uniformizing map and the $\mathrm{SLE}_8$ trace. *arXiv e-prints*, page arXiv :2107.03365, July 2021.

[61] K. Kavvadias, J. Miller, and L. Schoug. Conformal removability of $\mathrm{SLE}_4$. *arXiv e-prints*, page arXiv :2209.10532, Sept. 2022.

[62] K. Kavvadias, J. Miller, and L. Schoug. Conformal removability of non-simple Schramm-Loewner evolutions. *arXiv e-prints*, page arXiv :2302.10857, Feb. 2023.

[63] A. Kemppainen and S. Smirnov. Conformal invariance of boundary touching loops of FK Ising model. *Comm. Math. Phys.*, 369(1) :49–98, 2019.

[64] R. Kenyon. Conformal invariance of domino tiling. *Ann. Probab.*, 28(2) :759–795, 2000.

[65] R. Kenyon. Dominos and the Gaussian free field. *Ann. Probab.*, 29(3) :1128–1137, 2001.

[66] R. Kenyon, J. Miller, S. Sheffield, and D. B. Wilson. Six-vertex model and schramm-loewner evolution. *Phys. Rev. E*, 95 :052146, May 2017.

[67] R. Kenyon, J. Miller, S. Sheffield, and D. B. Wilson. Bipolar orientations on planar maps and $\mathrm{SLE}_{12}$. *Ann. Probab.*, 47(3) :1240–1269, 2019.

[68] V. G. Knizhnik, A. M. Polyakov, and A. B. Zamolodchikov. Fractal structure of 2D-quantum gravity. *Modern Phys. Lett. A*, 3(8) :819–826, 1988.

[69] A. Kupiainen, R. Rhodes, and V. Vargas. Integrability of Liouville theory : proof of the DOZZ formula. *Ann. of Math. (2)*, 191(1) :81–166, 2020.

[70] G. F. Lawler. *Conformally invariant processes in the plane*, volume 114 of *Mathematical Surveys and Monographs*. American Mathematical Society, Providence, RI, 2005.

[71] G. F. Lawler and M. A. Rezaei. Minkowski content and natural parameterization for the Schramm-Loewner evolution. *Ann. Probab.*, 43(3) :1082–1120, 2015.

[72] G. F. Lawler, O. Schramm, and W. Werner. Values of Brownian intersection exponents. I. Half-plane exponents. *Acta Math.*, 187(2) :237–273, 2001.

[73] G. F. Lawler, O. Schramm, and W. Werner. Values of Brownian intersection exponents. II. Plane exponents. *Acta Math.*, 187(2) :275–308, 2001.

[74] G. F. Lawler, O. Schramm, and W. Werner. Analyticity of intersection exponents for planar Brownian motion. *Acta Math.*, 189(2) :179–201, 2002.

[75] G. F. Lawler, O. Schramm, and W. Werner. Values of Brownian intersection exponents. III. Two-sided exponents. *Ann. Inst. H. Poincaré Probab. Statist.*, 38(1) :109–123, 2002.

[76] G. F. Lawler, O. Schramm, and W. Werner. Conformal invariance of planar loop-erased random walks and uniform spanning trees. *Ann. Probab.*, 32(1B) :939–995, 2004.

[77] G. F. Lawler, O. Schramm, and W. Werner. On the scaling limit of planar self-avoiding walk. In *Fractal geometry and applications : a jubilee of Benoît Mandelbrot, Part 2*, volume 72, Part 2 of *Proc. Sympos. Pure Math.*, pages 339–364. Amer. Math. Soc., Providence, RI, 2004.

[78] G. F. Lawler and S. Sheffield. A natural parametrization for the Schramm-Loewner evolution. *Ann. Probab.*, 39(5) :1896–1937, 2011.

[79] J.-F. Le Gall. The topological structure of scaling limits of large planar maps. *Invent. Math.*, 169(3) :621–670, 2007.

[80] J.-F. Le Gall. Geodesics in large planar maps and in the Brownian map. *Acta Math.*, 205(2) :287–360, 2010.

[81] J.-F. Le Gall. Uniqueness and universality of the Brownian map. *Ann. Probab.*, 41(4) :2880–2960, 2013.

[82] J.-F. Le Gall. Brownian geometry. *Jpn. J. Math.*, 14(2) :135–174, 2019.

[83] J.-F. Le Gall and G. Miermont. Scaling limits of random planar maps with large faces. *Ann. Probab.*, 39(1) :1–69, 2011.

[84] J.-F. Le Gall and F. Paulin. Scaling limits of bipartite planar maps are homeomorphic to the 2-sphere. *Geom. Funct. Anal.*, 18(3) :893–918, 2008.

[85] Y. Li, X. Sun, and S. S. Watson. Schnyder woods, SLE(16), and Liouville quantum gravity. *arXiv e-prints*, page arXiv :1705.03573, May 2017.

[86] J. R. Lind. Hölder regularity of the SLE trace. *Trans. Amer. Math. Soc.*, 360(7) :3557–3578, 2008.

[87] K. Löwner. Untersuchungen über schlichte konforme Abbildungen des Einheitskreises. I. *Math. Ann.*, 89(1-2) :103–121, 1923.

[88] J.-F. Marckert and A. Mokkadem. Limit of normalized quadrangulations : the Brownian map. *Ann. Probab.*, 34(6) :2144–2202, 2006.

[89] D. E. Marshall and S. Rohde. The Loewner differential equation and slit mappings. *J. Amer. Math. Soc.*, 18(4) :763–778, 2005.

[90] G. Miermont. On the sphericity of scaling limits of random planar quadrangulations. *Electron. Commun. Probab.*, 13 :248–257, 2008.

[91] G. Miermont. The Brownian map is the scaling limit of uniform random plane quadrangulations. *Acta Math.*, 210(2) :319–401, 2013.

[92] G. Miermont. *Aspects of random maps*. 2014.

[93] J. Miller and S. Sheffield. Imaginary geometry I : interacting SLEs. *Probab. Theory Related Fields*, 164(3-4) :553–705, 2016.

[94] J. Miller and S. Sheffield. Imaginary geometry II : reversibility of $\mathrm{SLE}_\kappa(\rho_1;\rho_2)$ for $\kappa \in (0,4)$. *Ann. Probab.*, 44(3) :1647–1722, 2016.

[95] J. Miller and S. Sheffield. Imaginary geometry III : reversibility of $\mathrm{SLE}_\kappa$ for $\kappa \in (4,8)$. *Ann. of Math. (2)*, 184(2) :455–486, 2016.

[96] J. Miller and S. Sheffield. Quantum Loewner evolution. *Duke Math. J.*, 165(17) :3241–3378, 2016.

[97] J. Miller and S. Sheffield. Imaginary geometry IV : interior rays, whole-plane reversibility, and space-filling trees. *Probab. Theory Related Fields*, 169(3-4) :729–869, 2017.

[98] J. Miller and S. Sheffield. Liouville quantum gravity spheres as matings of finite-diameter trees. *Ann. Inst. Henri Poincaré Probab. Stat.*, 55(3) :1712–1750, 2019.

[99] J. Miller and S. Sheffield. Liouville quantum gravity and the Brownian map I : the $\mathrm{QLE}(8/3,0)$ metric. *Invent. Math.*, 219(1) :75–152, 2020.

[100] J. Miller and S. Sheffield. An axiomatic characterization of the Brownian map. *J. Éc. polytech. Math.*, 8 :609–731, 2021.

[101] J. Miller and S. Sheffield. Liouville quantum gravity and the Brownian map II : Geodesics and continuity of the embedding. *Ann. Probab.*, 49(6) :2732–2829, 2021.

[102] J. Miller and S. Sheffield. Liouville quantum gravity and the Brownian map III : the conformal structure is determined. *Probab. Theory Related Fields*, 179(3-4) :1183–1211, 2021.

[103] J. Miller, S. Sheffield, and W. Werner. Non-simple conformal loop ensembles on Liouville quantum gravity and the law of CLE percolation interfaces. *Probab. Theory Related Fields*, 181(1-3) :669–710, 2021.

[104] J. Miller, S. Sheffield, and W. Werner. Simple conformal loop ensembles on Liouville quantum gravity. *Ann. Probab.*, 50(3) :905–949, 2022.

[105] J. Miller and H. Wu. Intersections of SLE paths : the double and cut point dimension of SLE. *Probab. Theory Related Fields*, 167(1-2) :45–105, 2017.

[106] R. C. Mullin. On the enumeration of tree-rooted maps. *Canadian J. Math.*, 19 :174–183, 1967.

[107] P. Nolin, W. Qian, X. Sun, and Z. Zhuang. Backbone exponent for two-dimensional percolation. *arXiv e-prints*, page arXiv :2309.05050, Sept. 2023.

[108] A. M. Polyakov. Quantum geometry of bosonic strings. *Phys. Lett. B*, 103(3) :207–210, 1981.

[109] A. M. Polyakov. Quantum geometry of fermionic strings. *Phys. Lett. B*, 103(3) :211–213, 1981.

[110] A. M. Polyakov. From Quarks to Strings. *arXiv e-prints*, page arXiv :0812.0183, Nov. 2008.

[111] R. Rhodes and V. Vargas. KPZ formula for log-infinitely divisible multifractal random measures. *ESAIM Probab. Stat.*, 15 :358–371, 2011.

[112] B. Rider and B. Virág. The noise in the circular law and the Gaussian free field. *Int. Math. Res. Not. IMRN*, (2) :Art. ID rnm006, 33, 2007.

[113] B. Rodin and D. Sullivan. The convergence of circle packings to the Riemann mapping. *J. Differential Geom.*, 26(2) :349–360, 1987.

[114] S. Rohde and O. Schramm. Basic properties of SLE. *Ann. of Math. (2)*, 161(2) :883–924, 2005.

[115] G. Schaeffer. *Conjugaison d'arbres et cartes combinatoires aléatoires*. PhD thesis, Université Bordeaux I, 1998.

[116] O. Schramm. Scaling limits of loop-erased random walks and uniform spanning trees. *Israel J. Math.*, 118 :221–288, 2000.

[117] O. Schramm and S. Sheffield. Contour lines of the two-dimensional discrete Gaussian free field. *Acta Math.*, 202(1) :21–137, 2009.

[118] O. Schramm and S. Sheffield. A contour line of the continuum Gaussian free field. *Probab. Theory Related Fields*, 157(1-2) :47–80, 2013.

[119] S. Sheffield. Gaussian free fields for mathematicians. *Probab. Theory Related Fields*, 139(3-4) :521–541, 2007.

[120] S. Sheffield. Exploration trees and conformal loop ensembles. *Duke Math. J.*, 147(1) :79–129, 2009.

[121] S. Sheffield. Conformal weldings of random surfaces : SLE and the quantum gravity zipper. *Ann. Probab.*, 44(5) :3474–3545, 2016.

[122] S. Sheffield. Quantum gravity and inventory accumulation. *Ann. Probab.*, 44(6) :3804–3848, 2016.

[123] S. Sheffield. What is a random surface ? *arXiv e-prints*, page arXiv :2203.02470, Mar. 2022.

[124] S. Sheffield and W. Werner. Conformal loop ensembles : the Markovian characterization and the loop-soup construction. *Ann. of Math. (2)*, 176(3) :1827–1917, 2012.

[125] S. Smirnov. Critical percolation in the plane : conformal invariance, Cardy's formula, scaling limits. *C. R. Acad. Sci. Paris Sér. I Math.*, 333(3) :239–244, 2001.

[126] S. Smirnov. Conformal invariance in random cluster models. I. Holomorphic fermions in the Ising model. *Ann. of Math. (2)*, 172(2) :1435–1467, 2010.

[127] S. Smirnov and W. Werner. Critical exponents for two-dimensional percolation. *Math. Res. Lett.*, 8(5-6) :729–744, 2001.

[128] K. Stephenson. Circle pack. http://www.circlepack.com/.

[129] A.-S. Sznitman. *Topics in occupation times and Gaussian free fields*. Zurich Lectures in Advanced Mathematics. European Mathematical Society (EMS), Zürich, 2012.

[130] T. Tao. Univalent functions, the Loewner equation, and the Bieberbach conjecture. https ://terrytao.wordpress.com/2018/05/02/246c-notes-3-univalent-functions-the-loewner-equation-and-the-bieberbach-conjecture/

[131] W. T. Tutte. A census of Hamiltonian polygons. *Canadian J. Math.*, 14 :402–417, 1962.

[132] W. T. Tutte. A census of planar triangulations. *Canadian J. Math.*, 14 :21–38, 1962.

[133] W. T. Tutte. A census of slicings. *Canadian J. Math.*, 14 :708–722, 1962.

[134] W. T. Tutte. A census of planar maps. *Canadian J. Math.*, 15 :249–271, 1963.

[135] M. Wang and H. Wu. Level lines of Gaussian free field I : Zero-boundary GFF. *Stochastic Process. Appl.*, 127(4) :1045–1124, 2017.

[136] W. Werner. Random planar curves and Schramm-Loewner evolutions. In *Lectures on probability theory and statistics*, volume 1840 of *Lecture Notes in Math.*, pages 107–195. Springer, Berlin, 2004.

[137] W. Werner and E. Powell. *Lecture notes on the Gaussian free field*, volume 28 of *Cours Spécialisés [Specialized Courses]*. Société Mathématique de France, Paris, 2021.

[138] D. Zhan. Reversibility of chordal SLE. *Ann. Probab.*, 36(4) :1472–1494, 2008.